Ab Initio Density Functional Theory Calculations and Vibrational Analysis of Zinc-Bound 4-Methylimidazole as a Model of a Histidine Ligand in Metalloenzymes†

Koji Hasegawa,*,§ Taka-aki Ono,§ and Takumi Noguchi*,‡

Laboratory for Photo-Biology (I), RIKEN Photodynamics Research Center, Aoba, Sendai, Miyagi 980-0845, Japan, and Biophysical Chemistry Laboratory, RIKEN, Wako, Saitama 351-0198, Japan

Received: June 15, 2001; In Final Form: September 20, 2001

Histidine is often found as a ligand in metalloenzymes. The imidazole side group has two nitrogen atoms capable of being protonated or of participating in metal binding. Hence, histidine can take on various metal-bound and protonated forms in proteins. Because of its variable structural state, histidine often functions as a key amino acid residue in enzymatic reactions. Raman and IR spectroscopies have been used as powerful methods to investigate the structure of histidine in proteins. In an attempt to establish the Raman and IR markers reflecting the coordinated and protonated states of histidine, we have calculated the optimized geometry and vibrational frequencies of various forms of zinc(II) complexes of 4-methylimidazole (4-MeIm), as a model of a histidine ligand, using the density functional theory (DFT) method. The effects of metal binding on the frequency and N-deuteration shift of the C4C5 stretching mode around 1600 cm^{-1} and of the C5N1 stretch around 1100 cm^{-1} were satisfactorily reproduced in calculation and explained by changes in the bond distances and the mixing of vibrations. Additionally, the calculated frequency of the Zn−imidazole stretching mode of neutral 4-MeIm at 260−255 cm^{-1} exhibited an upshift by ∼25 cm^{-1} upon its deprotonation, being consistent with the experimental observation. Furthermore, assignments were done for the several ring vibrations in the 1510−1250 cm^{-1} region that have previously been used as Raman markers of the metal-bound forms. The results provided a theoretical basis for use of these markers as a basis for determining the structure of histidine in proteins. Atomic charge calculations by the natural population analysis revealed that deprotonation of the MeIm ligand decreased the charge of the Zn^{2+} ion and decreased the acidity of the water ligands. This suggests a possible role of the histidine ligand in controlling the catalytic reactions of metalloenzymes by changing its protonation state.

Introduction

Histidine is commonly found as a ligand to the metal ions in metalloenzymes.[1,2] The imidazole (Im) ring of histidine possesses two nitrogen atoms (N1 and N3 in Figure 1), which can participate in metal binding, as well as become protonated. As a result, histidine can take on various metal-bound and protonated forms. There are four possible metal-free forms of histidine: the neutral N1H- and N3H-Im tautomers, the imidazolate anion (Im^-), and the imidazolium cation (ImH_2^+). Among these, the two neutral forms and the imidazolate anion can further bind a metal ion(s) at the unprotonated nitrogen site(s), producing five more metal-bound forms: N3M-N1H- and N1M-N3H-Im, and N3M-, N1M-, and M_2-Im^- (M = metal ion; Figure 1). Because of the myriad of forms histidine is capable of adopting, it is not surprising that it often functions as a versatile ligand that is directly involved in the catalytic reactions. For instance, in the reaction of Zn,Cu superoxide dismutase, it has been proposed that the coordination to the Cu ion of the metal-bridging histidine is first disrupted, and then a proton is taken up by this histidine and subsequently transferred to the superoxide anion.[3−6] In the heme−copper oxidases, a proton translocation mechanism that involves a histidine ligand of Cu_B has been proposed.[7,8] Thus, it is important to know the coordination and protonation state of a histidine ligand to understand the reaction mechanism of metalloenzymes.

Raman and IR spectroscopies have been used to investigate the histidine structures in proteins as well as in model compounds.[5,6,9−44] These vibrational spectroscopies are especially useful for identifying the coordination and protonation state of histidine because certain ring modes are highly sensitive to the difference in structural forms. Additionally, the metal−imidazole and N−H vibrations can be directly detected. Several empirical Raman and IR markers for the protonation and coordination structures of histidine have been developed. In Raman spectra, the C4C5 stretching bands have been observed at different frequencies: 1573−1565 and 1588−1580 cm^{-1} for the neutral N1H- and N3H-Im tautomers, respectively.[21,30] Miura et al.[30] further found that metal coordination upshifts both of the frequencies and gives bands at 1588−1573 and 1606−1594 cm^{-1} for the metal-bound N1H- and N3H-Im forms, respectively. In FTIR spectra, the C5N1 stretching bands around 1100 cm^{-1} exhibited different frequencies and N-deuteration shifts depending on the protonated forms.[34−36,44,45] However, the effect of metal coordination on this mode has not been studied in detail. Also, some Raman bands are known to intensify upon metal binding and have been used as convenient markers. For instance, the metal-bound N1H-Im form exhibits a strong band at ∼1275 cm^{-1}, and upon N-deuteration, intense bands at ∼1385 and

† Part of the special issue "Mitsuo Tasumi Festschrift".

* To whom correspondence should be addressed. E-mail for K.H.: kojihase@postman.riken.go.jp. E-mail for T.N.: tnoguchi@postman.riken.go.jp.

§ Laboratory for Photo-Biology (I).

‡ Biophysical Chemistry Laboratory.

10.1021/jp012251f CCC: $22.00
Published on Web 11/20/2001

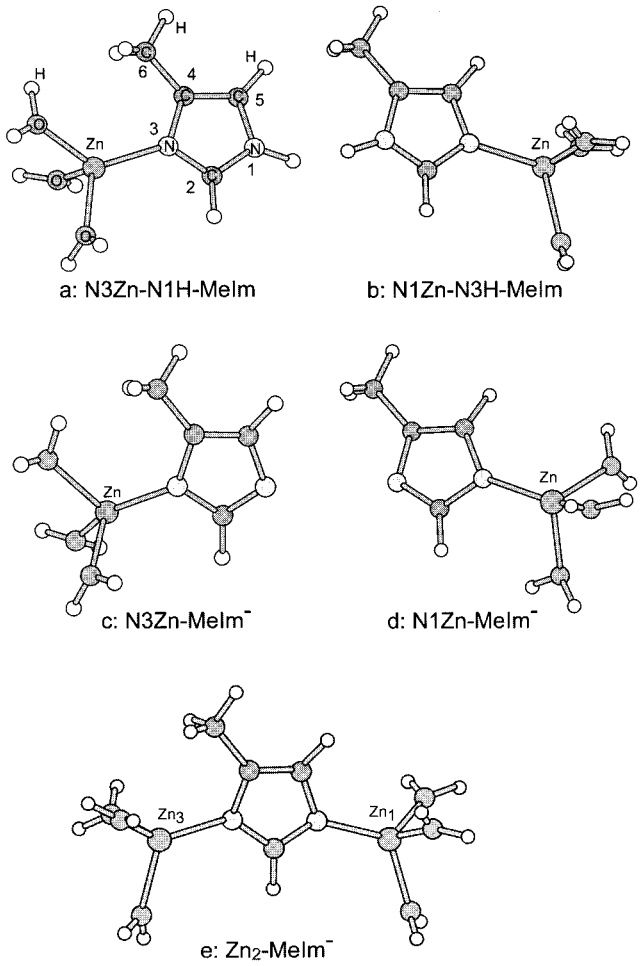

Figure 1. Optimized geometries of the model zinc(II) complexes of 4-methylimidazole in different protonation states. The imidazole ring in these complexes has the N3-Zn-bound, N1-protonated (N3Zn-N1H-MeIm) (a), N1-Zn-bound, N3-protonated (N1Zn-N3H-MeIm) (b), N3-Zn-bound imidazolate (N3Zn-MeIm$^-$) (c), N1-Zn-bound imidazolate (N1Zn-MeIm$^-$) (d), and N1,N3-Zn-bound imidazolate (Zn_2-MeIm$^-$) (e) forms. The Zn^{2+} center has tetrahedral coordination and the ligands other than 4-methylimidazole are water molecules. The same atom numbering (indicated in panel a) is used for all the five compounds.

$\sim$1265 cm^{-1} are observed.[6,22,30,32] On the other hand, in the metal-bound N3H-Im form, a strong band at $\sim$1430 cm^{-1} and a band at $\sim$1350 cm^{-1} upon N-deuteration are observed.[6,19,20,22,30−32,40] Furthermore, an intense band at $\sim$1290 cm^{-1} in the M_2-Im$^-$ form has been used as a marker of metal-bridging histidine in proteins.[5,6,18,27,33]

In a previous study,[45] we have performed ab initio vibrational analyses of various protonated forms of 4-methylimidazole (4-MeIm), a simple model compound of a histidine side chain, using the density functional theory (DFT) method. This provided the theoretical basis for utilizing Raman and IR markers as determinants of the protonation state of histidine. The calculated frequencies well reproduced the observed frequencies of the Raman and IR bands of 4-MeIm in aqueous solutions. The sensitivity of the frequencies and N-deuteration shifts of the markers to the protonation state was explained by the differences in optimized geometries and the coupling of vibrations. In this study, we have performed ab initio DFT calculations for various Zn-bound forms of 4-MeIm and investigated the metal-binding effect on the geometries, atomic charges, and vibrational frequencies of 4-MeIm in different protonated forms. Using the calculated results and the observed data in the literature, we theoretically analyze the Raman and IR markers as determinants of the coordination and protonation state of histidine and also discuss the possible role of the histidine ligand in metalloenzymes.

Computational Methods

The ab initio molecular orbital calculations were performed by the Gaussian 98 program package[46] on a Fujitsu 700E vector parallel computer in the Division of Computer and Information of RIKEN. Geometry optimizations were carried out by the DFT method using Becke's three parameter hybrid functional[47] combined with the Lee−Yang−Parr correlation functional (B3LYP)[48] with the 6-31G(df,p) basis set, except for Zn atoms, for which the Hay−Wadt effective core potential (LANL2DZ)[49] was used.

The Cartesian force constants were analytically computed at the fully optimized geometries. The obtained force-constant matrix was transformed from Cartesian to internal coordinates, and the vibrational frequencies and the potential energy distributions (PED) were calculated using the modified version of the NCTB program.[50,51] The internal coordinates of 4-MeIm were defined as those described by Majoube et al.[39] The three rotational modes of a water molecule coordinated to a Zn^{2+} ion, namely, wagging, rocking, and twisting modes, were defined in an analogous way as those of a methylene group. The three stretching and five deformation modes (consisting of two asymmetric and one symmetric deformation and two rocking modes) of the three water molecules attached to the Zn^{2+} ion ($Zn-(H_2O)_3$) were defined similarly to those of a methyl group.[52] For all the compounds, the computed frequencies were scaled with a uniform scaling factor of 0.98, which was determined in our previous calculations of various protonated forms of metal-free 4-MeIm.[45] The PED values (%) were normalized in each vibrational mode so that the sum of the PED equaled 100%.

Results

Five Zn complexes of 4-MeIm as shown in Figure 1 were used as model compounds for our calculation. These complexes cover all the possible metal-bound forms of 4-MeIm in different protonated states, namely, the N3−Zn-bound, N1-protonated form (N3Zn-N1H-MeIm, panel a), the N1−Zn-bound, N3-protonated form (N1Zn-N3H-MeIm, panel b), N3−Zn-bound imidazolate form (N3Zn-MeIm$^-$, panel c), N1−Zn-bound imidazolate form (N1Zn-MeIm$^-$, panel d), and the N1,N3−Zn-bound imidazolate form (Zn_2-MeIm$^-$, panel e) (Figure 1). Note that the imidazolium cation (N1,N3-protonated) form does not bind a metal ion. A divalent Zn cation was selected as the binding metal ion because (1) it has a closed shell so that the Zn^{2+}-MeIm complex has a singlet spin state, which renders the CPU resource minimum, and (2) there is abundant experimental data of vibrational spectra for Zn^{2+}-MeIm and Zn^{2+}-histidine complexes, and for Zn^{2+}-containing enzymes.[5,6,18,19,30,31,33] A tetrahedral coordination around the Zn^{2+} ion was assumed, with water molecules acting as ligands other than MeIm.

Metal-Binding Effects on the Optimized Geometries of Different Protonated Forms of 4-MeIm. The structures of the Zn^{2+}-MeIm complexes depicted in Figure 1 represent their optimized geometries obtained by the DFT calculation. Table 1 summarizes the selected geometrical parameters of each Zn-MeIm complex and the differences from those of the corresponding metal-free forms, which were previously calculated using the same method.[45] The metal-free N1H-MeIm has a rather asymmetric structure around the C2 atom, namely, a long N1−

TABLE 1: Optimized Geometry Parameters of Various Zn-Bound, Protonated Forms of 4-MeIm

	N3Zn-N1H-MeIm[a]	N1Zn-N3H-MeIm[b]	N3Zn-MeIm$^-$ [c]	N1Zn-MeIm$^-$ [c]	Zn_2-MeIm$^-$ [c]
			Distances (Å)		
N1−C2	1.3367 (−0.0274)	1.3376 (+0.0253)	1.3098 (−0.0389)	1.3771 (+0.0284)	1.3435 (−0.0052)
C2−N3	1.3413 (+0.0279)	1.3402 (−0.0282)	1.3821 (+0.0461)	1.3100 (−0.0400)	1.3472 (−0.0028)
N3−C4	1.4011 (+0.0178)	1.3871 (+0.0030)	1.3955 (+0.0039)	1.3830 (−0.0077)	1.3976 (+0.0248)
C4−C5	1.3660 (−0.0068)	1.3679 (−0.0053)	1.3718 (−0.0189)	1.3717 (−0.0190)	1.3657 (−0.0250)
C5−N1	1.3795 (−0.0023)	1.3973 (+0.0180)	1.3777 (+0.0055)	1.3982 (+0.0260)	1.3933 (+0.0211)
C4−C6	1.4934 (−0.0025)	1.4910 (−0.0015)	1.4949 (−0.0060)	1.4955 (−0.0054)	1.4946 (−0.0063)
N1−H	1.0125 (+0.0059)				
N3−H		1.0127 (+0.0055)			
C2−H	1.0793 (−0.0017)	1.0792 (−0.0018)	1.0844 (−0.0059)	1.0840 (−0.0063)	1.0805 (−0.0098)
C5−H	1.0782 (−0.0001)	1.0788 (−0.0021)	1.0810 (−0.0074)	1.0816 (−0.0068)	1.0796 (−0.0088)
Zn−N1		1.9953		1.9109	2.0056
Zn−N3	1.9978		1.9164		2.0068
Zn−O[d]	2.0596	2.0551	2.0904	2.0925	2.0613
O−H[e]	0.9692	0.9692	0.9681	0.9679	0.9695
			Angles (deg)		
N1C2N3	109.51 (−2.32)	109.47 (−2.28)	113.66 (−3.58)	113.63 (−3.61)	112.01 (−5.23)
C2N3C4	107.14 (+1.48)	109.94 (+2.38)	104.58 (+2.35)	105.60 (+3.37)	106.39 (+4.16)
N3C4C5	107.69 (−2.26)	104.60 (+0.34)	106.25 (−2.68)	109.21 (+0.28)	107.05 (+1.88)
C4C5N1	106.65 (+1.00)	109.60 (−1.86)	110.86 (−0.93)	107.58 (−2.35)	109.07 (−0.86)
C5N1C2	109.01 (+2.09)	106.38 (+1.41)	104.65 (+2.97)	103.98 (+2.30)	105.48 (+3.80)
N3C4C6	122.82 (+1.46)	123.16 (+0.02)	122.98 (−0.83)	121.48 (−0.67)	123.03 (+0.88)
C2N3Zn	127.04		127.04		130.17
C2N1Zn		127.87		128.36	132.20

[a] Values in parentheses are the differences from the parameters of the corresponding metal-free form (N1H-MeIm) obtained in our previous calculation.[45] [b] Values in parentheses are the differences from the parameters of the corresponding metal-free form (N3H-MeIm) obtained in our previous calculation.[45] [c] Values in parentheses are the differences from the parameters of the corresponding metal-free form (MeIm$^-$) obtained in our previous calculation.[45] [d] Average of the distances between Zn and the oxygen atoms of water ligands. [e] Average of the O−H distances of water ligands.

C2 bond (1.3641 Å) with a single-bond character and a short C2−N3 bond (1.3134 Å) with a double-bond character.[45] However, metal binding to the N3 atom shortened and lengthened the N1−C2 and C2−N3 bonds, respectively, by the similar amounts of 0.027−0.028 Å, resulting in the almost equivalent lengths (∼1.34 Å) of these bonds. A comparable effect, but with the opposite direction of change, was seen in the N3H-MeIm upon metal binding to the N1 atom; the lengthened N1−C2 and shortened C2−N3 bonds resulted in their similar lengths (∼1.34 Å). This symmetric structure around C2 is similar to the cases of $MeImH_2^+$ and MeIm$^-$,[45] although the N1−C2 and C2−N3 distances are slightly shorter in $MeImH_2^+$ (∼1.334 Å) and longer in MeIm$^-$ (∼1.35 Å). A previous calculation by Basch et al.[53] showed that when a naked Zn^{2+} atom is bound to imidazole, the change in the N1−C2 and C2−N3 distances is more prominent and the two distances are almost reversed. However, Cini et al.[54] showed that coordination of more ligands to the Zn^{2+} atom reduces this effect and makes the two bond distances similar, being consistent with our results.

In contrast to the neutral MeIm, binding of a single Zn^{2+} ion to MeIm$^-$ at the N1 or N3 site (Figure 1c,d) changed the N1−C2−N3 structure from a symmetric to an asymmetric one. N3Zn-MeIm$^-$ has a short N1−C2 distance (1.3098 Å) possessing double-bond character and a long C2−N3 distance (1.3821 Å) possessing single-bond character, whereas N1Zn-MeIm$^-$ has a long N1−C2 distance (1.3771 Å) and a short C2−N3 distance (1.3100 Å). The asymmetric tendency in these metal-bound imidazolate forms is more prominent than in the metal-free neutral N3H- and N1H-MeIm.[45] When two Zn^{2+} ions are bound to MeIm$^-$ at both the nitrogen sites (Zn_2-MeIm$^-$; Figure 1e), the N1−C2−N3 structure becomes symmetric again and shows slightly longer N1−C2 and C2−N3 distances (∼1.345 Å) than those of the Zn-bound N1H- and N3H-MeIm.

The single-bond character of the N3−C4 and C5−N1 bonds (1.38−1.40 Å) remained unchanged after metal binding in all the forms. These distances always increased when a Zn^{2+} ion is bound to the nitrogen atom in the bond. The C4−C5 distances decreased upon metal binding and gained more double-bond character in all the forms. The decrease was larger in MeIm$^-$ (0.018−0.025 Å) than in neutral MeIm (0.005−0.007 Å). The distances of the C4−C6 (C-Me) and C−H bonds all decreased upon metal binding, whereas the N−H distances increased in both the Zn-bound N1H-MeIm and N3H-MeIm complexes. The Zn−N distance was shorter by ∼0.08 Å in the single Zn^{2+} complexes of MeIm$^-$ (1.91−1.92 Å) than in the complexes of neutral MeIm (1.99−2.00 Å). On the other hand, the Zn−O distances of water ligands were longer by ∼0.03 Å in the former complexes (∼2.09 Å) than in the latter (2.055−2.06 Å). When two Zn^{2+} ions are bound to both the nitrogen sites of MeIm$^-$, both the Zn−N (2.00−2.01 Å) and Zn−O (∼2.061 Å) distances became slightly longer than those of the neutral forms.

The effect of metal binding on the inner angles of the imidazole ring displayed some common trends. Both the C2N3C4 and C5N1C2 angles increased by 1.4−4.2° upon Zn binding in all the forms. In contrast, the N1C2N3 angle always decreased by 2.2−5.3°.

Atomic Charges of the Zn-MeIm complexes. Table 2 presents the atomic charges of the Zn-MeIm complexes, obtained by the natural population analysis,[55,56] together with the differences from those of the corresponding metal-free forms of 4-MeIm. The largest change in the atomic charges of MeIm upon metal binding was observed at the nitrogen atom(s) of the binding site(s). The bound nitrogen was more negatively charged by ∼0.3 e, when a single Zn atom was bound to the neutral 4-MeIm or MeIm$^-$ anion. When two Zn atoms were bound to MeIm$^-$ at both the nitrogen sites, the charge decreased by ∼0.19 e at each nitrogen. The charges of the other atoms in the MeIm and MeIm$^-$ all increased upon Zn binding except for the methyl carbon (C6), for which the charge decreased in all cases.

TABLE 2: Atomic Charges (e) by the Natural Population Analysis of Various Zn-Bound, Protonated Forms of 4-MeIm

	N3Zn-N1H-MeIm[a]	N1Zn-N3H-MeIm[b]	N3Zn-MeIm$^-$ [c]	N1Zn-MeIm$^-$ [c]	Zn_2-MeIm$^-$ [c]
N1	−0.519 (+0.061)	−0.797 (−0.306)	−0.476 (+0.126)	−0.902 (−0.300)	−0.796 (−0.194)
C2	0.238 (+0.064)	0.239 (+0.072)	0.153 (+0.067)	0.161 (+0.075)	0.223 (+0.137)
N3	−0.793 (−0.294)	−0.524 (+0.057)	−0.897 (−0.291)	−0.481 (+0.125)	−0.796 (−0.190)
C4	0.139 (+0.038)	0.176 (+0.078)	0.078 (+0.055)	0.117 (+0.094)	0.138 (+0.115)
C5	−0.042 (+0.073)	−0.089 (+0.014)	−0.083 (+0.087)	−0.140 (+0.030)	−0.085 (+0.085)
C6	−0.742 (−0.034)	−0.741 (−0.021)	−0.726 (−0.043)	−0.711 (−0.028)	−0.741 (−0.058)
H (N1)	0.489 (+0.052)				
H (N3)		0.484 (+0.049)			
H (C2)	0.261 (+0.040)	0.261 (+0.040)	0.206 (+0.048)	0.204 (+0.046)	0.242 (+0.084)
H (C5)	0.290 (+0.054)	0.261 (+0.031)	0.240 (+0.068)	0.216 (+0.044)	0.260 (+0.088)
H (C6)[d]	0.269 (+0.025)	0.283 (+0.035)	0.240 (+0.034)	0.250 (+0.044)	0.269 (+0.063)
MeIm[e]	0.127 (+0.127)	0.118 (+0.118)	−0.786 (+0.214)	−0.784 (+0.216)	−0.748 (+0.252)
Zn	1.706	1.713	1.641	1.639	1.704/1.710[f]
O[g]	−1.073	−1.074	−1.053	−1.052	−1.075
H (O)[h]	0.564	0.565	0.550	0.550	0.565

[a] Values in parentheses are the differences from those of the corresponding metal-free form (N1H-MeIm), which were calculated in the optimized geometries obtained in our previous study.[45] [b] Values in parentheses are the differences from those of the corresponding metal-free form (N3H-MeIm), which were calculated in the optimized geometries obtained in our previous study.[45] [c] Values in parentheses are the differences from those of the corresponding metal-free form (MeIm$^-$), which were calculated in the optimized geometries obtained in our previous study.[45] [d] Average for the hydrogen atoms of CH_3. [e] Total charge of MeIm or MeIm$^-$. [f] Values for Zn1/Zn3. [g] Average for the oxygen atoms of water ligands. [h] Average for the hydrogen atoms of water ligands.

The total charge of MeIm increased upon Zn binding (Table 2). In other words, some negative charge was transferred to the Zn^{2+} ion from MeIm. The amount of charge transferred was 0.11−0.13 e for the neutral MeIm, and 0.21−0.22 e for the MeIm$^-$ anion when a single Zn atom is bound to either nitrogen atom (Table 2). This larger movement of negative charge (by ∼0.1 e) in the case of the MeIm$^-$ anion relative to the neutral form was also observed in the charge of the Zn atom. It was lower in the N3Zn-MeIm$^-$ and N1Zn-MeIm$^-$ complexes (∼1.64 e) than in the N3Zn-N1H-MeIm and N1Zn-N3H-MeIm (∼1.71 e) complexes. In Zn_2-MeIm$^-$, the change in the total charge of MeIm$^-$ was the largest (0.25 e). However, the similar charges of the two Zn ions (1.704 and 1.710 e) indicate that the transferred charge is evenly shared between the two Zn ions and the amount of the transferred charge for each Zn ion is similar to that in the complexes of neutral MeIm.

Water-ligand oxygen atoms are more negatively charged (by ∼0.02 e) and their hydrogen atoms are more positively charged (by ∼0.015 e) in N3Zn-N1H-MeIm, N1Zn-N3H-MeIm, and Zn_2-MeIm$^-$ than in N3Zn-MeIm$^-$ and N1Zn-MeIm$^-$ (Table 2). This indicates that the O−H bonds of the coordinated water molecules are more polarized in the former complexes.

Metal-Binding Effects on the Vibrational Modes of Different Protonated Forms of 4-MeIm. Tables 3−9 summarize the calculated vibrational frequencies and the assignments of N3Zn-N1H-MeIm, N3Zn-N1D-MeIm, N1Zn-N3H-MeIm, N1Zn-N3D-MeIm, N3Zn-MeIm$^-$, N1Zn-MeIm$^-$, and Zn_2-MeIm$^-$, together with the metal-induced shifts ($\Delta\nu_M$) from the frequencies of the corresponding modes of the metal-free forms.[45] The uniform scaling factor of 0.98, which was determined in our previous calculations of the metal-free forms of 4-MeIm, was used to directly compare the frequencies among the different metal-bound, protonated forms. Some observed frequencies of 4-MeIm or histidine complexes in the corresponding metal-bound, protonated forms are also included in the tables when they were available in the literature. The vibrations that exhibit characteristic changes upon metal binding are described in the following.

1. NH(D) Stretching Vibrations. The NH stretching frequencies of N1H-MeIm and N3H-MeIm that were calculated at 3600−3580 cm^{-1} in metal-free forms[45] downshifted by about 50 cm^{-1} upon Zn binding (Tables 3 and 5). Similarly, the ND stretching frequencies of the N-deuterated forms at ∼2640 cm^{-1} [45] also downshifted by about 30 cm^{-1} upon Zn binding (Tables 4 and 6). These downshifts are attributed to the increased N−H distances in the Zn-bound forms (Table 1).

2. CH Stretching Vibrations. Both the C2H and C5H stretching frequencies showed upshifts for all of the compounds upon Zn binding, resulting in the calculated values of 3243−3142 cm^{-1} (Tables 3−9). The extent of the upshift corresponds well to the decrease in the C−H distances (r_{CH}, Table 1): Zn_2-MeIm$^-$ ($\Delta\nu_M$ = +131−140 cm^{-1}; $-\Delta r_{CH}$ = 0.0088−0.0098 Å) > N3Zn-MeIm$^-$ ≈ N1Zn-MeIm$^-$ (+84−111 cm^{-1}; 0.0059−0.0074 Å) > N3Zn-N1H-MeIm ≈ N1Zn-N3H-MeIm (+22−35 cm^{-1}; 0.0001−0.0021 Å). No specific difference in the behavior between the C2H and C5H vibrations was found. The calculated frequencies, including those of the metal-free forms, are in the following order: $MeImH_2^+$ (3249−3243 cm^{-1}) > N3Zn-N1H-MeIm ≈ N1Zn-N3H-MeIm (3241−3222 cm^{-1}) > Zn_2-MeIm$^-$ (3212−3204 cm^{-1}) > N1H-MeIm ≈ N3H-MeIm (3219−3187 cm^{-1}) > N3Zn-MeIm$^-$ ≈ N1Zn-MeIm$^-$ (3192−3148 cm^{-1}) > MeIm$^-$ (3081−3064 cm^{-1}) (Tables 3−9; ref 45). This series indicates that protonation and metal binding have a similar effect on increasing the CH frequencies, although the former is more effective than the latter.

3. Ring Stretching Vibrations. The ring CC and CN stretching vibrations in the 1650−900 cm^{-1} region showed complex behaviors upon Zn binding. This is due to drastic changes in the bond distances and the ring symmetry (Table 1) and the resultant redistribution of the CC and CN stretches and the CH deformations. However, the C4C5 stretching mode calculated at 1615−1562 cm^{-1} (ν_7 in Tables 3−6; ν_6 in Tables 7−9), which has the highest frequencies in ring vibrations, showed rather simple behavior. In our calculation, the C4C5 frequencies upshifted largely (+19−72 cm^{-1}) upon Zn binding in all of the protonated forms. These upshifts are in agreement with the decreased C4−C5 distances upon Zn binding (Table 1). The frequencies, N-deuteration shifts, and metal-induced upshifts of this mode are useful for determining the coordination and protonation state of MeIm or histidine (see below).

Because the N1−C2 bond acquired double-bond character upon Zn binding to the N3 atom of MeIm$^-$ (Table 1), the second-highest frequency mode in the ring vibrations of N3Zn-MeIm$^-$ contains the major contribution of the N1C2 stretch

TABLE 3: Vibrational Frequencies (cm^{-1}) and Assignments for Zn-Bound, N1-Protonated 4-MeIm (N3Zn-N1H-MeIm)

	calculated		observed	
	ν^a	$\Delta\nu_M{}^b$	Zn−(DL-His)$_2{}^c$	assignment (PED)^d
ν_1	3548	−51		N1H st (99)
ν_2	3241	+22		C5H st (98)
ν_3	3226	+34		C2H st (98)
ν_4	3087	+29		CH_3 asym st (89), CH_3 sym st (11)
ν_5	3023	−12		CH_3 asym st (100)
ν_6	2969	−12		CH_3 sym st (87), CH_3 asym st (12)
ν_7	1604	+25	1580	C4C5 st (57), C4C6 st (12), C5H def (10)
ν_8	1516	+14	∼1500	C2H def (29), N1C2 st (28), C2N3 st (28)
ν_9	1470	+39	1488	N1H def (37), N1C2 st (20), C5N1 st (17)
ν_{10}	1454	−10		CH_3 asym def (86)
ν_{11}	1452	+3		CH_3 asym def (88)
ν_{12}	1397	+5		CH_3 sym def (89)
ν_{13}	1300	−26	1274	C2N3 st (32), N3C4 st (18), C5H def (12)
ν_{14}	1257	−11	1232	N3C4 st (33), C4C6 st (18), C5N1 st (13)
ν_{15}	1238	+13	1216	C5H def (34), C2H def (26), C2N3 st (15)
ν_{16}	1185	+73	1194	N1C2 st (38), N1H def (29), C2H def (23)
ν_{17}	1094	+19	1092	C5N1 st (52), C5H def (24), C2H def (8)
ν_{18}	1051	+5		CH_3 rock (77)
ν_{19}	1016	+62	1024	ring def 1 (32), ring def 2 (19), N3C4 st (13)
ν_{20}	981	−2	992	CH_3 rock (66), C4C5 st (9), ring def 1 (6)
ν_{21}	919	−7	914	ring def 1 (45), ring def 2 (21), N3C4 st (20)
ν_{22}	839	+115	826	C5H wag (45), C2H wag (28), ring tor 2 (10)
ν_{23}	798	−5		C2H wag (50), C5H wag (34), ring tor 2 (7)
ν_{24}	709	+207		N1H wag (79), C2H wag (9)
ν_{25}	655	+5		C4C6 st (32), ring def 2 (23), ring tor 1 (11)
ν_{26}	652	−22		ring tor 2 (30), ring tor 1 (29), C4C6 wag (17)
ν_{27}	622	−17		ring tor 1 (38), ring tor 2 (38), N1H wag (17)
ν_{28}	368	+38		C4C6 def (37), H_2O wag 1 (22), H_2O wag 3 (10)
ν_{29}	267	+6		C4C6 wag (66), ring tor 1 (10), Zn−Im wag (7)
ν_{30}	257			Zn−Im st (70)
ν_{31}	151	+46		CH_3 twist (40), H_2O twist 3 (26), Zn−Im wag (11)
ν_{32}	142			H_2O twist 1 (28), Zn−Im wag (22), H_2O twist 2 (18)
ν_{33}	129			Zn−Im def (41), Zn−$(H_2O)_3$ rock 1 (12)

[a] Only the frequencies of the modes involving the MeIm vibrations are selected. Calculated vibrational frequencies were scaled with a uniform scaling factor of 0.98. [b] Shifts from the calculated frequencies of metal-free N1H-MeIm.[45] [c] Frequencies from the Raman spectrum of crystalline bis(histidino)zinc(II) pentahydrate by Miura et al.[30] [d] Potential energy distributions are given in parentheses. Abbrevations for the internal coordinates: st, stretching; def, deformation; rock, rocking; wag, wagging; tor, torsion; twist, twisting; asym, asymmetric; sym, symmetric. Definitions of the ring deformation and torsion are followed by those in Majoube et al.[39]

TABLE 4: Vibrational Frequencies (cm^{-1}) and Assignments for Zn-Bound, N1-Deuterated 4-MeIm (N3Zn-N1D-MeIm)

	calculated		observed	
	ν^a	$\Delta\nu_M{}^b$	Zn−(DL-His)$_2{}^c$	assignment (PED)^d
ν_1	3242	+23		C5H st (98)
ν_2	3226	+33		C2H st (98)
ν_3	3087	+29		CH_3 asym st (89), CH_3 sym st (11)
ν_4	3023	−12		CH_3 asym st (99)
ν_5	2969	−12		CH_3 sym st (87), CH_3 asym st (12)
ν_6	2610	−34		N1D st (97)
ν_7	1596	+22	1571	C4C5 st (60), C4C6 st (14), C5H def (10)
ν_8	1510	+14	1495	C2H def (29), C2N3 st (29), N1C2 st (28)
ν_9	1454	−8		CH_3 asym def (83)
ν_{10}	1452	+3		CH_3 asym def (87)
ν_{11}	1402	+46	1389	CH_3 sym def (31), N1C2 st (21), C5N1 st (12)
ν_{12}	1395	+3		CH_3 sym def (56), C5N1 st (14), $N1C_2$ st (13)
ν_{13}	1296	−26	1259	C2N3 st (35), N3C4 st (18), C5H def (11)
ν_{14}	1249	−15	1226	N3C4 st (29), C4C6 st (20), C5N1 st (19)
ν_{15}	1233	+11	1208	C2H def (43), C5H def (34), C2N3 st (13)
ν_{16}	1114	+35	1105	C5N1 st (31), N1C2 st (22), C5H def (15)
ν_{17}	1051	+5		CH_3 rock (74)
ν_{18}	1049	(+86)	1044	ring def 1 (25), ring def 2 (13), N3C4 st (10)
ν_{19}	983	−19	970	CH_3 rock (63), ring def 1 (10), C4C5 st (6)
ν_{20}	908	−8	901	ring def 1 (40), ring def 2 (24), N3C4 st (19)
ν_{21}	866	+38		N1D def (68), ring def 1 (11)
ν_{22}	835	+111	822	C5H wag (51), C2H wag (26), ring tor 2 (10)
ν_{23}	797	−6		C2H wag (56), C5H wag (28), ring tor 2 (9)
ν_{24}	655	−15		ring tor 2 (33), ring tor 1 (31), C4C6 wag (17)
ν_{25}	652	+4		C4C6 st (35), ring def 2 (26), ring tor 2 (9)
ν_{26}	622	+7		ring tor 1 (38), ring tor 2 (38), N1D wag (17)
ν_{27}	529	+139		N1D wag (94)
ν_{28}	367	+40		C4C6 def (33), H_2O wag 1 (22), H_2O wag 3 (10)
ν_{29}	262	+4		C4C6 wag (66), ring tor 1 (10), Zn−Im wag (9)
ν_{30}	255			Zn−Im st (68)
ν_{31}	150	+45		CH_3 twist (41), H_2O twist 3 (26), Zn−Im wag (11)
ν_{32}	142			H_2O twist 1 (27), Zn−Im wag (23), H_2O twist 2 (18)
ν_{33}	129			Zn−Im def (41), Zn−$(H_2O)_3$ rock 1 (12), H_2O twist 1 (9)

[a] Only the frequencies of the modes involving the MeIm vibrations are selected. Calculated vibrational frequencies were scaled with a uniform scaling factor of 0.98. [b] Shifts from the calculated frequencies of metal-free N1D-MeIm.[45] The parentheses imply that the mode shape is not well-conserved after metal binding. [c] Frequencies from the Raman spectrum of crystalline N-deuterated bis(histidino)zinc(II) pentahydrate by Miura et al.[30] [d] Potential energy distributions are given in parentheses. Abbrevations for the internal coordinates: st, stretching; def, deformation; rock, rocking; wag, wagging; tor, torsion; twist, twisting; asym, asymmetric; sym, symmetric. Definitions of the ring deformation and torsion are followed by those in Majoube et al.[39]

(1485 cm^{-1}; ν_7 in Table 7). The comparable mode in N1Zn-MeIm$^-$ (1487 cm^{-1}; ν_7 in Table 8) is contributed predominantly by the C2N3 bond, which acquired double-bond character upon Zn binding at N1 (Table 1). The same tendency was seen in the metal-free N3H-MeIm and N1H-MeIm,[45] in which the N1C2 and C2N3 stretches, consisting of double-bond character,

TABLE 5: Vibrational Frequencies (cm^{-1}) and Assignments for Zn-Bound, N3-Protonated 4-MeIm (N1Zn-N3H-MeIm)

	calculated		observed		
	ν^a	$\Delta\nu_M{}^b$	Co(4-MeIm)$_6{}^c$	Cu−(βAla-His)^d	assignment (PED)^e
ν_1	3543	−45			N3H st (99)
ν_2	3228	+35			C2H st (93)
ν_3	3222	+35			C5H st (93)
ν_4	3098	+31			CH_3 asym st (96)
ν_5	3059	+49			CH_3 asym st (100)
ν_6	2999	+33			CH_3 sym st (95)
ν_7	1615	+21	1593	1594	C4C5 st (47), C4C6 st (13), N3H def (12)
ν_8	1518	+24	1490	1503	N1C2 st (31), C2H def (34), C2N3 st (25)
ν_9	1460	−1	1455		CH_3 asym def (64), C2N3 st (8)
ν_{10}	1447	−6	1455		CH_3 asym def (91)
ν_{11}	1414	+11	1425	1434	N3H def (25), C4C5 st (15), CH_3 asym def (14)
ν_{12}	1402	+9	1392		CH_3 sym def (80)
ν_{13}	1329	−25	1346	1335	N1C2 st (30), N3C4 st (26), ring def 2 (12)
ν_{14}	1276	+19	1258	1274	C5H def (50), C2N3 st (11), C5N1 st (10)
ν_{15}	1231	−4	1232	1224	C2H def (28), C5N1 st (24), N1C2 st (14)
ν_{16}	1155	+64	1154	1173	N3H def (34), C2N3 st (23), C5H def (13)
ν_{17}	1108	−18	1112	1112	C5N1 st (55), C5H def (12), C2H def (10)
ν_{18}	1046	+2			CH_3 rock (74)
ν_{19}	1014	+6	1013	1014	CH_3 rock (27), ring def 2 (24), C4C5 st (17)
ν_{20}	972	+7			ring def 1 (41), CH_3 rock (36), N3C4 st (10)
ν_{21}	963	+53	954	939	ring def 1 (30), ring def 2 (24), N3C4 st (20)
ν_{22}	819	+32		839	C2H wag (61), C5H wag (17), ring tor 2 (15)
ν_{23}	791	−41			C5H wag (61), C2H wag (15), ring tor 1 (11)
ν_{24}	708	+193			N3H wag (83), C2H wag (8)
ν_{25}	653	+6			C4C6 st (44), ring def 2 (33)
ν_{26}	651	+14			ring tor 1 (43), ring tor 2 (35)
ν_{27}	634	−34			ring tor 2 (38), ring tor 1 (29), C4C6 wag (17)
ν_{28}	339	+22			C4C6 def (73)
ν_{29}	270	+25			C4C6 wag (58), ring tor 1 (13), Zn−Im wag (11)
ν_{30}	260				Zn−Im st (78)
ν_{31}	152				Zn−Im def (50), Zn−$(H_2O)_3$ rock 1 (18)
ν_{32}	130				Zn−Im wag (39), CH_3 twist (29), Zn−$(H_2O)_3$ rock 2 (20)
ν_{33}	108	−17			CH_3 twist (66), C4C6 wag (9)

[a] Only the frequencies of the modes involving the MeIm vibrations are selected. Calculated vibrational frequencies were scaled with a uniform scaling factor of 0.98. [b] Shifts from the calculated frequencies of metal-free N3H-MeIm.[45] [c] Frequencies from the Raman spectrum of crystalline hexakis(4-methylimidazole)cobalt(II) chloride by Itabashi and Itoh.[22] [d] Frequencies from the Raman spectrum of crystalline (β-alanyl-L-histidino)copper(II) dihydrate by Miura et al.[30] [e] Potential energy distributions are given in parentheses. Abbrevations for the internal coordinates: st, stretching; def, deformation; rock, rocking; wag, wagging; tor, torsion; twist, twisting; asym, asymmetric; sym, symmetric. Definitions of the ring deformation and torsion are followed by those in Majoube et al.[39]

showed the second-highest frequencies in the ring vibrations (calculated at 1494 and 1502 cm^{-1}, respectively). The rather symmetric geometry of the N1−C2−N3 moiety in N3Zn-N1H-MeIm, N1Zn-N3H-MeIm, and Zn_2-MeIm$^-$ (Table 1) makes the mode pattern of the N1−C2 and C2−N3 stretches similar to that of $MeImH_2{}^+$.[45] The N1−C2 and C2−N3 stretches are coupled with each other, and with additional mixing of the C2H deformation, relatively high-frequency modes are produced at 1518−1510 cm^{-1} in N3Zn-N1H(D)-MeIm and N1Zn-N3H(D)-MeIm (ν_8 in Tables 3−6) and at 1491 cm^{-1} in Zn_2-MeIm (ν_7 in Table 9). These modes correspond to the vibration calculated at 1537 cm^{-1} (1534−1533 cm^{-1} in observation) in $MeImH_2{}^+$.[45]

The three to four modes in the 1360−1150 cm^{-1} region are due to mixing of the various CN stretches and CH and NH deformations. Upon Zn binding, redistribution of these vibrations occurred and the mode shapes changed appreciably from those of the corresponding metal-free form, especially in the Zn-bound MeIm$^-$ complexes.

The modes with a major contribution of the C5N1 vibration, which were calculated at 1132−1091 cm^{-1} (ν_{17} in Tables 3 and 5; ν_{16} in Tables 4 and 6; ν_{15} in Tables 7−9), were basically conserved after metal binding. However, frequency changes upon metal binding were rather complex. The calculated frequencies of N1H-MeIm and N3H-MeIm upshifted by 19 cm^{-1} and downshifted by 18 cm^{-1}, respectively, upon Zn binding. Upon binding of Zn to MeIm$^-$ at N3 and N1, the C5N1 frequencies upshifted by 12 cm^{-1} and downshifted by 29 cm^{-1}, respectively, while Zn binding to both nitrogen sites induced a slight downshift by 5 cm^{-1}. This cannot be explained simply by the changes in the C5−N1 distance (Table 1). Nevertheless, differences in the frequencies and the N-deuteration shifts make this mode a useful marker reflecting the coordination and protonation state (see below).

4. Mixed Modes of the Ring Deformation, CH_3 Rocking, and C4C5 and N3C4 Stretching Vibrations. Three modes occur in the 1060−900 cm^{-1} region originating from the mixing of the ring deformation, CH_3 rocking, and C4C5 and N3C4 stretching vibrations (Tables 3−9, the nearly pure CH_3 rocking mode at 1051−1041 cm^{-1} is excluded). The origins of these modes in the metal-free forms are the two modes calculated at 1015−954 cm^{-1} due to the same mixing as detailed above, and a mode at 936−910 cm^{-1} due to the nearly pure ring deformations.[45] Upon binding Zn, the mixing of these vibrations changes dramatically. In the metal-free forms, the mixed mode of the CH_3 rock, ring deformations, and C4C5 stretch observed around 1000 cm^{-1} is known to depend on the protonation state.[21] This mode was the highest in frequency among the three modes in the metal-free forms.[45] However, in N3Zn-N1H(D)-MeIm, N3Zn-MeIm$^-$ and Zn_2-MeIm$^-$, the mode mainly due to the ring deformations (ν_{19} in Table 3, ν_{18} in Table 4, ν_{16} in Table 7, and ν_{17} in Table 9) is found at 1053−1016 cm^{-1}, above the corresponding mixed mode at ∼1000 cm^{-1}. A similar ring

TABLE 6: Vibrational Frequencies (cm^{-1}) and Assignments for Zn-Bound, N3-Deuterated 4-MeIm (N1Zn-N3D-MeIm)

	calculated		observed	
	ν^a	$\Delta\nu_M{}^b$	Cu−(βAla-His)[c]	assignment (PED)[d]
ν_1	3228	+34		C2H st (93)
ν_2	3222	+35		C5H st (93)
ν_3	3098	+31		CH_3 asym st (96)
ν_4	3059	+49		CH_3 asym st (100)
ν_5	2999	+33		CH_3 sym st (95)
ν_6	2606	−30		N3D st (97)
ν_7	1598	+19	1570	C4C5 st (55), C4C6 st (15), C5H def (10)
ν_8	1512	+21	1495	N1C2 st (32), C2H def (29), C2N3 st (24)
ν_9	1454	−6		CH_3 asym def (77)
ν_{10}	1447	−6		CH_3 asym def (91)
ν_{11}	1403	+7		CH_3 sym def (89)
ν_{12}	1357	+35	1349	C2N3 st (34), N3C4 st (23), C4C5 st (13)
ν_{13}	1324	−40	1327	N1C2 st (34), N3C4 st (18), ring def 2 (11)
ν_{14}	1261	+7	1254	C5H def (58), C2H st (14), C5N1 st (12)
ν_{15}	1230	+10	1231	C2H def (30), C5N1 st (22), N1C2 st (12)
ν_{16}	1109	−16	1108	C5N1 st (55), C5H def (15), C2H def (8)
ν_{17}	1046	+2		CH_3 rock (74)
ν_{18}	1011	+11	996	CH_3 rock (50), ring def 2 (18), C4C5 st (14)
ν_{19}	986	(+24)		ring def 1 (46), N3D def (12)
ν_{20}	962	+48	958	ring def 2 (27), N3C4 st (26), ring def 1 (16)
ν_{21}	881	+30		N3D def (60), ring def 1 (17)
ν_{22}	818	+32	821	C2H wag (58), C5H wag (22), ring tor 2 (15)
ν_{23}	787	−44		C5H wag (58), C2H wag (23), ring tor 1 (10)
ν_{24}	653	−12		ring tor 1 (47), ring tor 2 (34)
ν_{25}	646	+7		C4C6 st (41), ring def 2 (33)
ν_{26}	634	+18		ring tor 2 (39), ring tor 1 (25), N3D wag (16)
ν_{27}	526	+127		N3D wag (95)
ν_{28}	334	+22		C4C6 def (74)
ν_{29}	268	+24		C4C6 wag (58), ring tor 1 (13), Zn−Im wag (10)
ν_{30}	258			Zn−Im st (78)
ν_{31}	152			Zn−Im def (50), Zn−$(H_2O)_3$ rock 1 (19)
ν_{32}	129			Zn−Im wag (39), CH_3 twist (29), Zn−$(H_2O)_3$ rock 2 (21)
ν_{33}	108	−16		CH_3 twist (66)

[a] Only the frequencies of the modes involving the MeIm vibrations are selected. Calculated vibrational frequencies were scaled with a uniform scaling factor of 0.98. [b] Shifts from the calculated frequencies of metal-free N3D-MeIm.[45] The parentheses imply that the mode shape is not well-conserved after metal binding. [c] Frequencies from the Raman spectrum of crystalline N-deuterated (β-alanyl-L-histidino)copper(II) dihydrate by Miura et al.[30] [d] Potential energy distributions are given in parentheses. Abbrevations for the internal coordinates: st, stretching; def, deformation; rock, rocking; wag, wagging; tor, torsion; twist, twisting; asym, asymmetric; sym, symmetric. Definitions of the ring deformation and torsion are followed by those in Majoube et al.[39]

deformation mode is observed at much lower frequency of 976−962 cm^{-1} in N1Zn-N3H(D)-MeIm and N1Zn-MeIm$^-$ (ν_{21} in Table 5, ν_{20} in Table 6, and ν_{18} in Table 8).

5. C-Me Stretching Vibration. The C-Me (C4−C6) stretching mode was calculated at 665−646 cm^{-1} (ν_{25} in Tables 3−6; ν_{23} in Tables 7−8; ν_{22} in Table 9). The frequencies increased slightly upon Zn binding (3−13 cm^{-1}), reflecting the decreased distances of the C4−C6 bonds.

TABLE 7: Vibrational Frequencies (cm^{-1}) and Assignments for the Zn(N3)-Bound Imidazolate Form of 4-MeIm (N3Zn-MeIm$^-$)

	calculated		
	ν^a	$\Delta\nu_M{}^b$	assignment (PED)[c]
ν_1	3192	+111	C5H st (99)
ν_2	3148	+84	C2H st (99)
ν_3	3068	+79	CH_3 asym st (81), CH_3 sym st (18)
ν_4	2941	+10	CH_3 asym st (97)
ν_5	2907	0	CH_3 sym st (78), CH_3 asym st (20)
ν_6	1562	+48	C4C5 st (53), C4C6 st (14), C5H def (11)
ν_7	1485	+4	CH_3 asym def (34), N1C2 st (27), C2H def (15)
ν_8	1457	+13	CH_3 asym def (74), N1C2 st (10)
ν_9	1453	+13	CH_3 asym def (56), N1C2 st (16)
ν_{10}	1381	+10	CH_3 sym def (87)
ν_{11}	1357	+58	N3C4 st (27), N1C2 st (23), C5N1 st (12)
ν_{12}	1262	+46	C2H def (32), C5H def (19), N3C4 st (12)
ν_{13}	1248	−6	C5H def (28), C5N1 st (25), N3C4 st (19)
ν_{14}	1182	(−51)	C2N3 st (68), C2H def (12)
ν_{15}	1132	+12	C5N1 st (59), C5H def (20), ring def 2 (7)
ν_{16}	1053	+64	ring def 1 (30), ring def 2 (21), Zn−Im st (16)
ν_{17}	1045	+12	CH_3 rock (83)
ν_{18}	965	+8	CH_3 rock (69), C4C5 st (10)
ν_{19}	903	−33	ring def 1 (53), ring def 2 (23), N3C4 st (13)
ν_{20}	849	+98	C5H wag (86), ring tor 1 (11)
ν_{21}	777	−19	C2H wag (84), ring tor 2 (15)
ν_{22}	661	−28	ring tor 2 (75), ring tor 1 (20)
ν_{23}	655	+3	C4C6 st (46), ring def 2 (32)
ν_{24}	628	−35	ring tor 1 (60), C4C6 wag (21), ring tor 2 (13)
ν_{25}	382	+62	C4C6 def (40), Zn−Im st (26), Zn−$(H_2O)_3$ sym st (11)
ν_{26}	280		Zn−Im st (44), C4C6 def (17), Zn−$(H_2O)_3$ sym st (14)
ν_{27}	250	−3	C4C6 wag (72)
ν_{28}	199	+99	CH_3 twist (81)
ν_{29}	135		Zn−Im def (70)
ν_{30}	108		Zn−Im wag (32), Zn−$(H_2O)_3$ rock 2 (27), Zn−$(H_2O)_3$ rock 1 (13)

[a] Only the frequencies of the modes involving the MeIm vibrations are selected. Calculated vibrational frequencies were scaled with a uniform scaling factor of 0.98. [b] Shifts from the calculated frequencies of metal-free MeIm$^-$.[45] The parentheses imply that the mode shape is not well-conserved after metal binding. [c] Potential energy distributions are given in parentheses. Abbrevations for the internal coordinates: st, stretching; def, deformation; rock, rocking; wag, wagging; tor, torsion; twist, twisting; asym, asymmetric; sym, symmetric. Definitions of the ring deformation and torsion are followed by those in Majoube et al.[39]

6. Zn−Im Stretching Vibration. In N3Zn-N1H(D)-MeIm and N1Zn-N3H(D)-MeIm, the Zn−Im stretching frequencies were calculated at 260−255 cm^{-1} (ν_{30} in Tables 3−6), while in N3Zn- and N1Zn-MeIm$^-$, they were higher by about 25 cm^{-1} and calculated at 286−280 cm^{-1} (ν_{26} in Tables 7 and 8). These higher frequencies are attributed to the shorter Zn−N(Im) distances (Table 1). In Zn_2-MeIm$^-$, the Zn1−Im and Zn3−Im vibrations were coupled with each other and split into the two modes at 305 cm^{-1} (asymmetric stretch) and 199 cm^{-1} (symmetric stretch) (ν_{26} and ν_{28} in Table 9).

Discussion

Raman and IR Markers of the Coordination and Protonation State of Histidine. To date, various Raman and IR markers of coordination and protonation state of the imidazole ring of histidine have been proposed and used to determine the structural conformation of histidine in proteins. In the following, using the calculated results of the Zn-MeIm complexes in this study together with the experimental data in the literature, we will theoretically analyze these markers and discuss their applicability.

TABLE 8: Vibrational Frequencies (cm^{-1}) and Assignments for the Zn(N1)-Bound Imidazolate Form of 4-MeIm ($N1Zn\text{-}MeIm^-$)

	calculated		
	ν^a	$\Delta\nu_M{}^b$	assignment (PED)[c]
ν_1	3173	+92	C5H st (99)
ν_2	3151	+87	C2H st (100)
ν_3	3065	+76	CH_3 asym st (99)
ν_4	3045	+114	CH_3 asym st (100)
ν_5	2989	+82	CH_3 sym st (99)
ν_6	1568	+54	C4C5 st (54), C4C6 st (16), C5H def (10)
ν_7	1487	(+47))	C2N3 st (43), C2H def (23), N1C2 st (9)
ν_8	1460	−21	CH_3 asym def (74), C2N3 st (12)
ν_9	1449	+5	CH_3 asym def (92)
ν_{10}	1396	+25	CH_3 sym def (87)
ν_{11}	1333	(+117)	C2N3 st (32), N3C4 st (16), C2H def (11)
ν_{12}	1274	−25	N3C4 st (35), ring def 2 (13), C4C6 st (12)
ν_{13}	1232	−22	C5H def (43), C2H def (38)
ν_{14}	1205	−28	C5N1 st (44), N1C2 st (40), ring def 1 (9)
ν_{15}	1091	−29	C5N1 st (30), C5H def (24), N1C2 st (24)
ν_{16}	1045	+12	CH_3 rock (77)
ν_{17}	998	(+9)	CH_3 rock (39), ring def 2 (24), C4C5 st (18)
ν_{18}	976	+40	ring def 1 (51), ring def 2 (13), Zn−Im st (12)
ν_{19}	957	(0)	ring def 1 (27), N3C4 st (26), CH_3 rock (23)
ν_{20}	788	−8	C2H wag (79), ring tor 2 (13)
ν_{21}	708	−43	C5H wag (67), ring tor 1 (15), C2H wag (10)
ν_{22}	666	−23	ring tor 2 (43), ring tor 1 (30), C4C6 wag (20)
ν_{23}	661	+9	C4C6 st (42), ring def 1 (32), ring def 1 (10)
ν_{24}	633	−30	ring tor 1 (47), ring tor 2 (38), C4C6 wag (9)
ν_{25}	341	+21	C4C6 def (61), Zn−$(H_2O)_3$ sym st (16)
ν_{26}	286		Zn−Im st (49), Zn−$(H_2O)_3$ sym st (21)
ν_{27}	262	+9	C4C6 wag (63), ring tor 1 (14)
ν_{28}	146		H_2O twist 2 (29), H_2O twist 3 (19), Zn−Im def (14)
ν_{29}	133		H_2O twist 2 (35), H_2O twist 1 (16), Zn−Im def (13)
ν_{30}	114	+14	CH_3 twist (84)

[a] Only the frequencies of the modes involving the MeIm vibrations are selected. Calculated vibrational frequencies were scaled with a uniform scaling factor of 0.98. [b] Shifts from the calculated frequencies of metal-free $MeIm^-$.[45] The parentheses imply that the mode shape is not well-conserved after metal binding. [c] Potential energy distributions are given in parentheses. Abbrevations for the internal coordinates: st, stretching; def, deformation; rock, rocking; wag, wagging; tor, torsion; twist, twisting; asym, asymmetric; sym, symmetric. Definitions of the ring deformation and torsion are followed by those in Majoube et al.[39]

1. C4C5 Stretching Vibration. The C4C5 stretching vibration has been used as a good marker of the protonation state, as well as metal binding.[6,21,22,30−33,39,45] Table 10 summarizes the calculated C4C5 frequencies of the various Zn-bound, protonated forms of 4-MeIm and the observed frequencies of the corresponding forms of 4-MeIm or histidine found in the literature. For the neutral forms, metal-free 4-MeIm in aqueous solution shows two bands at 1575 and 1594 cm^{-1}, which are due to the tautomeric equilibrium of N1H-MeIm and N3H-MeIm, respectively.[39,45] The higher frequency by 15−20 cm^{-1} in the N3H form than in the N1H form has also been observed for free histidine in aqueous solution, for which the bands at 1573−1565 and 1588−1580 cm^{-1} have been obtained.[21,30] Miura et al.[30] reported that metal binding to histidine resulted in upshifts of the C4C5 frequencies in both forms. The collected experimental data in Table 10 show that the extent of the metal-induced upshift is 0−20 cm^{-1} and bands are found at 1590−1573[6,30,32,33] and 1606−1593[22,30−33] cm^{-1} in the metal-bound N1H-Im and N3H-Im forms, respectively. Compared with the neutral forms, the imidazolate anion form of $MeIm^-$ has a much lower C4C5 frequency in the free state (1535 cm^{-1}).[45] Metal binding to both of the nitrogen sites of the Im^- form upshifts the frequency by 26−30 cm^{-1} and results in bands appearing at 1564−1555 cm^{-1}.[5,6,33]

TABLE 9: Vibrational Frequencies (cm^{-1}) and Assignments for the Zn(N1,N3)-Bound Imidazolate Form of 4-MeIm ($Zn_2\text{-}MeIm^-$)

	calculated		observed	
	ν^a	$\Delta\nu_M{}^b$	Zn−$(4\text{-}MeIm^-)_2$[c]	assignment (PED)[d]
ν_1	3212	+131		C5H st (95)
ν_2	3204	+140		C2H st (95)
ν_3	3087	+98		CH_3 asym st (90)
ν_4	3029	+98		CH_3 asym st (99)
ν_5	2977	+70		CH_3 sym st (88)
ν_6	1586	+72	1558	C4C5 st (59), C4C6 st (14), C5H def (11)
ν_7	1491	(+51)		C2H def (31), N1C2 st (24), C2N3 st (21)
ν_8	1451	−30		CH_3 asym def (89)
ν_9	1446	+2		CH_3 asym def (75)
ν_{10}	1399	+28		CH_3 sym def (90)
ν_{11}	1314	+15	1343	N1C2 st (40), N3C4 st (18), ring def 2 (10)
ν_{12}	1291	(+37)	1283	C2N3 st (36), N3C4 st (16), C5H def (15)
ν_{13}	1244	(+28)	1250	C5H def (34), C2H def (33), C2N3 st (18)
ν_{14}	1234	+1	∼1233	C5N1 st (26), N3C4 st (16), N1C2 st (16)
ν_{15}	1115	−5	1108	C5N1 st (54), C5H def (18), C2H def (8)
ν_{16}	1041	+8		CH_3 rock (73)
ν_{17}	1039	+50	1047	ring def 1 (28), ring 2 def (17), N3C4 st (11)
ν_{18}	986	+29	977	CH_3 rock (51), ring def 1 (24), ring def 2 (7)
ν_{19}	957	+21		ring def 1 (27), N3C4 st (23), ring def 2 (20)
ν_{20}	817	+21		C2H wag (43), C5H wag (37), ring tor 2 (13)
ν_{21}	791	+40		C5H wag (43), C2H wag (41), ring tor 1 (7)
ν_{22}	665	+13		C4C6 st (45), ring def 2 (27), N3C4 st (8)
ν_{23}	658	−31		ring tor 2 (77)
ν_{24}	648	−15		ring tor 1 (68), C4C6 wag (20)
ν_{25}	380	+60		C4C6 def (36), H_2O wag 1 (13), H_2O wag 3 (11)
ν_{26}	305			Zn1−Im st (34), Zn3−Im st (34)
ν_{27}	281	+28		C4C6 wag (54), Zn3−Im wag (15), Zn1−Im wag (11)
ν_{28}	199			Zn3−Im st (37), Zn1−Im st (28)
ν_{29}	161			Zn1−Im wag (31), H_2O twist 1 (13), Zn3−Im wag (10)
ν_{30}	157			H_2O twist 6 (21), Zn3−Im def (17), H_2O twist 5 (10)
ν_{31}	126			H_2O twist 3 (21), Zn1−Im def (18), Zn1−$(H_2O)_3$ sym def (11)
ν_{32}	113			Zn3−$(H_2O)_3$ rock 2 (17), Zn3−Im wag (17), H_2O twist 5 (11)
ν_{33}	95	−5		CH_3 twist (53)

[a] Only the frequencies of the modes involving the MeIm vibrations are selected. Calculated vibrational frequencies were scaled with a uniform scaling factor of 0.98. [b] Shifts from the calculated frequencies of metal-free $MeIm^-$.[45] The parentheses imply that the mode shape is not well-conserved after metal binding. [c] Frequencies from the Raman spectrum of polymeric adducts of zinc(II) with 4-methylimidazole by Hashimoto et al.[6] [d] Potential energy distributions are given in parentheses. Abbrevations for the internal coordinates: st, stretching; def, deformation; rock, rocking; wag, wagging; tor, torsion; twist, twisting; asym, asymmetric; sym, symmetric. Definitions of the ring deformation and torsion are followed by those in Majoube et al.[39]

Our previous calculations well reproduced the observed C4C5 frequencies as well as their N-deuteration shifts for all the metal-free forms of 4-MeIm.[45] This present study showed that the binding of Zn to neutral N1H-MeIm and N3H-MeIm upshifted

TABLE 10: Calculated and Observed Frequencies (cm^{-1}) of the C4C5 Stretching Mode of Various Metal-bound, Protonated Forms of 4-MeIm or Histidine

site of metal and proton							
N1	N3		ν	$\Delta\nu_M$[a]	$\Delta\nu_D$[b]	assignment (PED)[c]	ref
			N1H-Im				
H		calculated (N1H-MeIm)	1579		−5	C4C5 st (55), C4C6 st (14), C5H def (10), C2N3 st (4), N1H def (4)	45
		4-MeIm in H_2O[d]	1575		−6		45
H	M	calculated (N3Zn-N1H-MeIm)	1604	+25	−8	C4C5 st (57), C4C6 st (12), C5H def (10), N1H def (6)	this work
		Zn−(DL−His)$_2$	1580	+7	−9		30
		Ni−(DL−His)$_2$	1573	0	−10		30
		Cu-GGH	1588	+17	−7		30
		Cu−HGG	1588	nd	−7		30
		Cu−PHGGG	1590	+16	−6		32
		Cu,Zn−SOD (red)[e]	1590	nd	−15		6
		Cu-Aβ_{1-16}[f]	1588	nd	nd		33
			N3H-Im				
	H	calculated (N3H-MeIm)	1594		−15	C4C5 st (44), C4C6 st (14), N3H def (10), C5H def (10)	45
		4-MeIm in H_2O[d]	1594		−19		45
M	H	calculated (N1Zn-N3H-MeIm)	1615	+21	−17	C4C5 st (47), C4C6 st (13), N3H def (12), C5H def (9)	this work
		Co(4-MeIm)$_6$	1593	nd	nd		22
		Cu−(βAla-His)	1594	+6	−24		30
		Zn−(zinc finger)[g]	1606	+20	−20		30, 31
		Zn-Aβ[h]	1604	nd	−20		33
		Cu−OP2 (pH 6)[i]	1603	nd	−19		32
			Im^-				
		calculated ($MeIm^-$)	1514			C4C5 st (45), C4C6 st (14), C5H def (13)	45
		$MeIm^-$ in NaOH[d]	1535				45
	M	calculated (N3Zn-$MeIm^-$)	1562	+48		C4C5 st (53), C4C6 st (14), C5H def (11)	this work
M		calculated (N1Zn-$MeIm^-$)	1568	+54		C4C5 st (54), C4C6 st (16), C5H def (10)	this work
M	M	calculated (Zn_2-$MeIm^-$)	1586	+72		C4C5 st (59), C4C6 st (14), C5H def (11)	this work
		Zn−(4-$MeIm^-$)$_2$	1558	+26[k]			6
		Zn−(His^-)$_2$	1560	+30[l]			6
		Cu,Zn−SOD[j]	1564−1562	nd			5,6
		Zn-Aβ[h]	1555	nd			33
			ImH_2^+				
H	H	calculated ($MeImH_2^+$)	1636		−24	C4C5 st (47), N3H def (12), C4C6 st (11), C2H def (8), N1H def (6)	45
		$MeImH_2^+$ in HCl[d]	1633		−28		45

[a] Shifts from the frequencies of the corresponding metal-free compounds. [b] Shifts upon N-deuteration. [c] Potential energy distributions are given in parentheses. Abbrevations for the internal coordinates: st, stretching; def, deformation; rock, rocking; wag, wagging; tor, torsion; twist, twisting; asym, asymmetric; sym, symmetric. Definitions of the ring deformation and torsion are followed by those in Majoube et al.[39] [d] Data from the FTIR spectra of 4-MeIm in aqueous solutions. [e] His 61 of reduced Cu,Zn-superoxide dismutase. [f] Soluble complex of Cu(II) and the N-terminal 16-residue fragment of the 40-residue human amyloid β-peptide. [g] Aqueous solution of a 27-mer zinc finger peptide in the presence of $ZnCl_2$. [h] Insoluble aggregates precipitated from the mixture of Zn(II) and the 40-residue human amyloid β-peptide or its N-terminal 16-residue fragment. [i] Aqueous solution of OP2 ((PHGGGWGQ)$_2$) in the presence of Cu(II) at pH 6. [j] His 61 of native Cu,Zn-superoxide dismutase. [k] Calculated using the Raman data of 4-$MeIm^-$ in aqueous solution by Hasegawa et al.[45] [l] Calculated using the Raman data of His^- in aqueous solution by Hashimoto et al.[27]

the C4C5 frequencies by 25 and 21 cm^{-1}, respectively, yielding frequencies of 1604 and 1615 cm^{-1} in N3Zn-N1H-MeIm and N1Zn-N3H-MeIm, respectively. Additionally, the binding of Zn to the $MeIm^-$ anion at N3, N1, and both nitrogen sites induced upshifts of the C4C5 frequencies by 48, 54, and 72 cm^{-1} with resultant frequencies of 1562, 1568, and 1586 cm^{-1}, respectively. Thus, the upshifts of the C4C5 stretching frequencies upon metal binding were reproduced in our calculations, although the extent of the upshifts and the resultant frequencies were a little too large compared with the experimental values. In our calculations, a strong correlation was observed between the frequency shift and the decrease in the C4−C5 distance (r_{C4C5}) upon Zn binding (Table 1): Zn_2-$MeIm^-$ ($\Delta\nu = 72$ cm^{-1}; $-\Delta r_{C4C5} = 0.0248$ Å) > N1Zn-$MeIm^-$ (54 cm^{-1}; 0.0190 Å) > N3Zn-$MeIm^-$ (48 cm^{-1}; 0.0189 Å) > N3Zn-N1H-MeIm (25 cm^{-1}; 0.0068 Å) > N1Zn-N3H-MeIm (21 cm^{-1}; 0.0053 Å). The larger upshifts and higher frequencies present in our calculations compared with the experimental values might be due to the choice in scaling factor. We used the scaling factor as determined in our previous calculations of the metal-free forms. However, the best scaling factor for the Zn-MeIm complexes might be slightly different because of the much larger size of the system or the presence of the metal ion. Although no observed C4C5 frequencies were found for the N3M-Im^- and N1M-Im^- forms in the literature, the values are expected to fall between ~1560 (M_2-Im^-) and ~1535 (metal-free $MeIm^-$) cm^{-1} because of the calculated frequency order of Zn_2-$MeIm^-$ > N1Zn-$MeIm^-$ > N3Zn-$MeIm^-$ > free $MeIm^-$.

TABLE 11: Calculated and Observed Frequencies (cm^{-1}) of the C5N1 Stretching Mode of Various Metal-bound, Protonated Forms of 4-MeIm or Histidine

site of metal and proton							
N1	N3		ν	$\Delta\nu_M$[a]	$\Delta\nu_D$[b]	assignment (PED)[c]	ref
			N1H-Im				
H		calculated (N1H-MeIm)	1075		+4	C5N1 st (44), C5H def (27), N1H def (7)	45
		4-MeIm in H_2O[d]	1087		+10		45
H	M	calculated (N3Zn-N1H-MeIm)	1094	+19	+20	C5N1 st (52), C5H def (24), C2H def (8), N1H def (6)	this work
		Zn−(DL-His)$_2$	1092	+1	+13		30
		Ni−(DL-His)$_2$	1096/1084[e]	−1	+3/+15		30
			N3H-Im				
	H	calculated (N3H-MeIm)	1126		−1	C5N1 st (57), C5H def (15), C2H def (8)	45
		4-MeIm in H_2O[d]	1104		0		45
M	H	calculated (N1Zn-N3H-MeIm)	1108	−18	+1	C5N1 st (55), C5H def (12), C2H def (10)	this work
		Co(4-MeIm)$_6$	1112	nd	nd		22
		Cu−(βAla-His)	1112	+7	0		30
		FePP(4-MeIm)$_2$ (pH 8)[f]	1103	−2	0		34
		Cyt*b*559(ox)[g]	1104	nd	nd		34
		PSII Fe^{2+}/Fe^{3+}[h]	1111−1110/1103−1102	nd	−1/+1		35, 36, 41
		PSII OEC[i]	1114−1113	nd	0		44
			Im^-				
		calculated ($MeIm^-$)	1120		0	C5N1 st (38), C5H def (31), N1C2 st (9)	45
		$MeIm^-$ in NaOH[d]	1101		0		45
	M	calculated (N3Zn-$MeIm^-$)	1132	+12		C5N1 st (59), C5H def (20), ring def 2 (7)	this work
M		calculated (N1Zn-$MeIm^-$)	1091	−29		C5N1 st (30), C5H def (24), N1C2 st (24)	this work
		FePP(4-MeIm)$_2$ (pH 12)[j]	1099	nd	nd		34
		PSII Fe^{3+}[k]	1094	nd	−1		35, 36
M	M	calculated (Zn_2-$MeIm^-$)	1115	−5		C5N1 st (54), C5H def (18), C2H def (8)	this work
		Zn−(4-$MeIm^-$)$_2$	1108	nd			6
		Zn−(His^-)$_2$	1118	nd			6
			ImH_2^+				
H	H	calculated ($MeImH_2^+$)	1081		+22	C5N1 st (54), C5H def (19), N1H def (8)	45
		$MeImH_2^+$ in HCl[d]	1088		+18		45

[a] Shifts from the frequencies of the corresponding metal-free compounds. [b] Shifts upon N-deuteration. [c] Potential energy distributions are given in parentheses. Abbrevations for the internal coordinates: st, stretching; def, deformation; rock, rocking; wag, wagging; tor, torsion; twist, twisting; asym, asymmetric; sym, symmetric. Definitions of the ring deformation and torsion are followed by those in Majoube et al.[39] [d] Data from the FTIR spectra of 4-MeIm in aqueous solutions. [e] Doublet probably due to Fermi resonance. [f] Bis(4-methylimidazole) complex of iron protoporphyrin in H_2O at pH 8. [g] Oxidized form of isolated cytochrome *b*559 of photosystem II. [h] The non-heme iron of photosystem II. [i] The oxygen-evolving complex of photosystem II. [j] Bis(4-methylimidazole) complex of iron protoporphyrin in H_2O at pH 12. [k] The oxydized non-heme iron of photosystem II.

In the metal-free neutral forms, the C4C5 frequencies show downshifts upon N-deuteration (Table 10). As discussed in our previous paper,[45] this is due to decoupling of the NH deformation vibration from the C4C5 stretching mode by the NH/ND exchange. Upon metal binding, the experimentally observed downshifts by N-deuteration seem to increase slightly. The ND-shift ($\Delta\nu_D$) of free N1H-MeIm in aqueous solution is -6 cm^{-1},[45] while in various metal−histidine complexes in the N3M−N1H-Im form, it is observed between -6 and -15 cm^{-1} (Table 10).[6,30,32] Also, the observed ND-shift of metal-free N3H-MeIm is -19 cm^{-1},[45] while the metal complexes of this form have values between -19 and -24 cm^{-1}.[22,30−33] This pattern was well reproduced in our calculation. The calculated ND-shifts of -5 and -15 cm^{-1} for metal-free N1H-MeIm and N3H-MeIm became -8 and -17 cm^{-1}, respectively, upon Zn binding (Table 10). These ND-shifts can be readily explained in terms of mixing of the NH deformation. In metal-free N1H-MeIm, the N1H deformation has 4% PED, which increased slightly to 6% upon Zn binding (Table 10). Additionally, the metal-free N3H-MeIm has 10% PED of the N3H deformation, and this value increased to 12% in the Zn-bound N3H-MeIm.

Thus, absolute frequencies of the C4C5 stretching mode and their ND-shifts can be used to differentiate each metal-bound, protonated form. The frequency order is expected to be ImH_2^+ ($\sim$1630 cm^{-1}) > N1M-N3H-Im (1610−1590 cm^{-1}) $\geq$ N3H-Im (1595−1580 cm^{-1}) $\geq$ N3M-N1H-Im (1590−1570 cm^{-1}) $\geq$ N1H-Im (1575−1565 cm^{-1}) > M_2-Im^- ($\sim$1560 cm^{-1}) > N3M-Im^- $\sim$ N1M-Im^- (1560−1535 cm^{-1}) > Im^- ($\sim$1535 cm^{-1}). Furthermore, the magnitude of the downshift upon N-deuteration ($-\Delta\nu_D$) is ImH_2^+ ($\sim$30 cm^{-1}) > N1M-N3H-Im (20−25 cm^{-1}) $\geq$ N3H-Im ($\sim$20 cm^{-1}) > N3M-N1H-Im (5−15 cm^{-1}) $\geq$ N1H-Im ($\sim$5 cm^{-1}) > N1M-, N3M-, and M_2-Im^- (0 cm^{-1}).

2. C5N1 Stretching Vibration. The rather isolated C5N1 stretching band observed around 1100 cm^{-1} has been used as a marker of the protonation state of histidine especially in FTIR studies.[34−36,44,45] Table 11 summarizes the observed and calculated C5N1 stretching frequencies for various metal-bound,

protonated forms of MeIm or histidine. Experimental data show that metal-free MeIm in aqueous solution has bands at 1087 and 1104 cm^{-1} arising from neutral N1H-MeIm and N3H-MeIm, respectively.[45] The higher C5N1 frequency of the N3H form by 17 cm^{-1} relative to the N1H form is similar to the case of the C4C5 frequencies discussed above. Upon metal binding, slight upshifts ($\leq$10 cm^{-1}) of the C5N1 frequencies are seen both in the N1H-Im and N3H-Im forms, and the bands are observed at ~1090 and 1114−1102 cm^{-1} in the metal-bound N1H-Im and N3H-Im forms, respectively[22,30,34−36,41,44] (Table 11). Thus, the experimental relationship that the C5N1 frequency is higher in N3H-Im by 10−20 cm^{-1} relative to that of N1H-Im holds even in the metal-bound forms. On the other hand, when a metal ion is bound to the Im^- anionic form, the observed metal-free frequency at 1101 cm^{-1} ($MeIm^-$ in NaOH solution) downshifts slightly, yielding an observed frequency at 1099−1094 cm^{-1} in the N1M-Im^- form,[34−36] whereas the frequency upshifts to 1118−1108 cm^{-1} in the M_2-Im^- form[6] (Table 11). No experimental data was found for the N3M-Im^- form.

It is seen in Table 11 that the calculated frequencies for the Zn-bound forms of MeIm well reproduce the aforementioned experimentally observed frequencies. However, the calculated metal-induced shifts ($\Delta\nu_M$) are in disagreement with the observed ones. This is due to the fact that some of the calculated frequencies of metal-free forms of MeIm are rather different from the observed ones (by 12, 22, and 19 cm^{-1} in N1H-MeIm, N3H-MeIm, and $MeIm^-$, respectively), although the order of the frequencies reflects the observations.[45]

The calculated ND-shifts ($\Delta\nu_D$) of the C5N1 frequencies agree well with the observed ones in both the metal-free and metal-bound forms (Table 11). In the N1H-Im form, the upshifts by ~10 cm^{-1} were observed in both the metal-free and metal-bound states. In the calculations, the upshifts by 4 and 20 cm^{-1} were predicted in metal-free and Zn-bound N1H-MeIm, respectively. On the other hand, the N3H-Im form shows little ND-shifts in both the metal-free and metal-bound states (Table 11). The difference in the sensitivity to N-deuteration is attributed to the extent of mixing of the NH deformation in this mode. In N1H-MeIm, the N1H deformation has 6−7% PED in both the metal-free and metal-bound states, whereas N3H-MeIm has almost no contribution from the N3H deformation in both states. In contrast to the C4C5 stretching mode, mixing of the NH vibration pushes down the C5N1 frequency (because the frequency of the original NH deformation is higher than that of the C5N1 stretch), and hence, decoupling of the NH vibration by N-deuteration upshifts the C5N1 frequency of N1H-MeIm. Despite the similar PED value of the NH deformation (6−7%), the calculated upshift of Zn-bound N1H-MeIm (20 cm^{-1}) was much larger than that of the metal-free form (4 cm^{-1}). After decoupling of the NH vibration, the PED values of the C5N1 stretch decrease from 44% to 28% in metal-free N1H-MeIm and from 52% to 31% in its Zn-bound form, while the N1C2 stretch is additionally mixed to this mode (22%−32%) (ref 45; Tables 3 and 4). Such redistribution of vibrations upon NH decoupling might account for the discrepancy in the calculated ND-shift between the metal-free and Zn-bound N1H-MeIm.

Thus, the C5N1 stretching mode can be useful in determining the coordination and protonation state of histidine. For the neutral forms, the N3H-Im form has a higher frequency than the N1H-Im form, by 10−20 cm^{-1}, both in the free and in the metal-bound states. The band is observed in the 1095−1085 cm^{-1} region for the N1H-Im and in the 1115−1100 cm^{-1} region for the N3H-Im. Because metal binding seems to increase the frequency slightly, the higher parts of these regions might reflect the metal-bound forms. Additionally, measuring the ND-shift can readily differentiate between the neutral N1H-Im and N3H-Im forms. An upshift of about 10 cm^{-1} will be indicative of the N1H form, whereas no shift will be observed in the N3H form. This relationship holds even after metal binding.

Deprotonation of the metal-bound neutral Im forms can be detected by the frequency shift of the C5N1 mode. Berthomieu, Hienerwadel and co-workers[34−36] previously observed the downshift of the C5N1 band by 4−9 cm^{-1} for the metal-bound N3H-Im form when it is deprotonated to yield the N1M-Im^- form. Our calculation predicted a slightly larger downshift of 17 cm^{-1} (Table 11). Also, an increase in the IR intensity of this mode upon deprotonation has been reported.[34] The calculated IR intensity was 58 km/mol in Zn-bound N3H-MeIm and 82 km/mol in N1Zn-$MeIm^-$, being consistent with the experimental observations. For the Zn-bound N1H-form, on the other hand, a large upshift of 38 cm^{-1} upon deprotonation was predicted by our calculations (Table 11). The calculated frequency of the resultant N3Zn-$MeIm^-$ is 1132 cm^{-1}, the highest in all the forms. Hence, it will be easy to differentiate this form. Experimental data are necessary to confirm this prediction. The M_2-Im^- form has a similar frequency as the metal-bound N3H-Im form (~1110 cm^{-1}), and both show no ND-shift. Hence, it might be difficult to differentiate these two structures only by the C5N1 stretching mode.

3. Mixed Mode of Ring Deformation, CH_3 Rocking, and C4C5 Stretching Vibrations. The band around 1000 cm^{-1} due to the mixed mode of the ring deformation, CH_3 rock, and C4C5 stretch has been shown to be dependent on the protonation state of metal-free 4-MeIm or histidine.[21,45] The corresponding modes were calculated at 981(983), 1014(1011), 965, 998, and 986 cm^{-1} for N3Zn-N1H(D)-MeIm, N1Zn-N3H(D)-MeIm, N3Zn-$MeIm^-$, N1Zn-$MeIm^-$, and Zn_2-$MeIm^-$, respectively (Tables 3−9). The effect of metal binding was considerable on the extent of mixing of each vibration in this mode. Nevertheless, in the neutral forms, the higher frequency in N3H-MeIm relative to N1H-MeIm (1013 and 995 cm^{-1}, observed; 1008 and 983 cm^{-1}, calculated[45]) was conserved after Zn binding (1014−1013 and 992 cm^{-1}, observed; 1014 and 981 cm^{-1}, calculated; Tables 3 and 5). The ND-shifts, on the other hand, changed considerably upon metal binding. They were calculated to be −3 and +2 cm^{-1} in Zn-bound N3H-MeIm and N1H-MeIm, respectively (Tables 3−6), compared with −8 and +19 cm^{-1} in metal-free N3H-MeIm and N1H-MeIm,[45] respectively. Although one might think that the higher frequency of N3H-MeIm could discriminate between these two neutral forms, the appearance of the ring deformation mode at 1016 cm^{-1} (observed at 1024 cm^{-1}) in Zn-bound N1H-MeIm (ν_{19} in Table 3) tends to make the band identification difficult. These results, together with the significant contribution of the CH_3 vibration, which is replaced with the CH_2 vibration in histidine, suggest that this mode is not suitable for practical use as a marker of the histidine structure. It is interesting to note the presence of the ring deformation mode at 1053−1039 cm^{-1} in N3Zn-N1D-MeIm (ν_{18} in Table 4), N3Zn-$MeIm^-$ (ν_{16} in Table 7), and Zn_2-$MeIm^-$ (ν_{17} in Table 9). This frequency region is higher than that of the mixed mode (1020−960 cm^{-1}) and could be used as a marker reflecting metal binding because in this region only the pure CH_3 rocking mode, which is inactive in resonance Raman spectra, is found in metal-free forms.[45] In fact, Hashimoto et al.[6] and Wang et al.[5] observed a band at 1050 cm^{-1} in the UV resonance Raman spectra of Cu,Zn−SOD, which was assigned to the histidine (His 61) bridging the $Zn^{2+}$and Cu^{2+} ions. Wang et al.[5] further found another band at 1050 cm^{-1} in D_2O solution, which was

TABLE 12: Other Ring Vibrations as Raman Markers of Metal-Binding and Protonation State of 4-MeIm or Histidine

N3M-N1H-Im

	ν_H[a] (ν_D[b])	ν_D[b]	ν_H[a]	ref
		Observed		
Zn−(DL-His)$_2$	1274 (1259)	1389		30
Ni−(DL-His)$_2$	1274 (1262)	1381	1503	30
Zn−(L-His)$_2$	(1269)	1385		6
Ni−(L-His)$_2$	1272			22
Cu−GlyHis	(1264)	1388		6
Cu−GGH	1276 (1266)	1387		30
Cu−HGG	1277 (1267)	1390		30
Cu−PHGGG	1274 (1268)	1394	1502	32
		Calculated		
N3Zn-N1H-MeIm	1300 (1296)	1402	1516	this work
assignment (PED)[c]	C2N3 st (32), N3C4 st (18), C5H def (12)	CH_3 sym def (31), N1C2 st (21), C5N1 st (12)	C2H def (29), N1C2 st (28), C2N3 st (28)	

N1M-N3H-Im

	ν_H	ν_D	ν_H	ref
		Observed		
Co(4-MeIm)$_6$	1425			22
Cu−(βAla-His)	1434	1349	1503	6, 30
Zn−(βAla-His)	1440		1503	40
Cu−OP2 (pH 6.0)[d]		1352		32
Zn−(zinc finger)[e]		1342	1503	30, 31
Zn−CP1[f]		1343		19
Cd−CP1[g]		1341		19
microperoxidase[h]		1343		20
hemoglobin		1340		20
		Calculated		
N1Zn-N3H-MeIm	1414	1357	1518	this work
assignment (PED)[c]	N3H def (25), C4C5 st (15), CH_3 asym def (14)	C2N3 st (34), N3C4 st (23), C4C5 st (13)	N1C2 st (31), C2H def (34), C2N3 st (25)	

M_2-Im^-

	ν	ref
	Observed	
Zn−($MeIm^-$)$_2$	1283	6
Zn−(His^-)$_2$	1287	6
Cu,Zn−SOD[i]	1292−1290/1282	5, 6, 18, 27
Zn-Aβ[j]	1290	33
	Calculated	
Zn_2-$MeIm^-$	1291	this work
assignment (PED)[c]	C2N3 st (36), N3C4 st (16), C5H def (15)	

[a] Frequencies in N-protonated forms. [b] Frequencies in N-deuterated forms. [c] Potential energy distributions are given in parentheses. Abbrevations for the internal coordinates: st, stretching; def, deformation; rock, rocking; wag, wagging; tor, torsion; twist, twisting; asym, asymmetric; sym, symmetric. Definitions of the ring deformation and torsion are followed by those in Majoube et al.[39] [d] Aqueous solution of OP2 ((PHGGGWGQ)$_2$) in the presence of Cu(II) at pH 6. [e] Aqueous solution of a 27-mer zinc finger peptide in the presence of $ZnCl_2$. [f] Zn(II)-bound CP1 (a consensus peptide designed based on C_2H_2-type zinc fingers: PYKCP ECGKSFSRKS DLVKH RRTHTG). [g] Cd(II)-bound CP1. [h] *N*-Acetyl microperoxidase-8 and microperoxidase-11. [i] His 61 of native Cu,Zn-superoxide dismutase. The doublet was interpreted as being due to Fermi resonance by Hashimoto et al.[6] and due to different two modes by Wang et al.[5] [j] Insoluble aggregates precipitated from the mixture of Zn(II) and 40-residue human amyloid β-peptide or its N-terminal 16-residue fragment.

tentatively assigned to the histidine ligand (His 69) of the Zn^{2+} ion in the N1D-Im form.

4. Other Ring Stretching Vibrations as Raman Markers of Metal Binding. It has been reported that some ring stretching vibrations of metal-bound histidine gain strong Raman intensities and hence can be useful Raman markers of metal binding.[5,6,18−20,22,27,30−33,40] Table 12 summarizes such Raman markers together with the calculated frequencies and assignments. So far, only the bands in the metal-bound N1H-Im and N3H-Im forms and the metal-bridging Im^- form (M_2-Im^-) have been studied. Some bands are enhanced only in N-deuterated forms (expressed as ν_D in Table 12).

The metal-bound N1H-Im form shows a strong Raman band at 1277−1272 cm^{-1} and at 1269−1259 cm^{-1} in its ND-form[6,22,30,32] (Table 12). This band has been considered to originate from the band at 1288−1282 cm^{-1} in metal-free histidine or at 1304−1301 cm^{-1} in metal-free 4-MeIm, which has been assigned to the "ring-breathing" mode.[21,22,30] In our previous work[45] the 1301 cm^{-1} band of N1H-MeIm was assigned to the mixed mode of the C2N3, N3C4, and C5N1 stretching vibrations with a calculated value of 1326 cm^{-1}. The corresponding mode in Zn-bound N1H-MeIm was calculated at 1300 cm^{-1} (ν_{13} in Table 3) with the contribution of the C2N3 (32%) and N3C4 (18%) stretches and the C5H deformation

(12%). The calculated frequency was slightly downshifted to 1296 cm^{-1} upon N-deuteration. The observed downshift by ~10 cm^{-1} upon metal binding and a further ~10 cm^{-1} downshift upon N-deuteration were qualitatively reproduced in our calculations represented by the downshifts of 26 and 4 cm^{-1} upon metal-binding and N-deuteration, respectively.

The almost identical modes of the C2N3 and N3C4 stretches also appeared in Zn-bound N3D-MeIm (ν_{12} in Table 6), Zn_2-$MeIm^-$ (ν_{12} in Table 9), and N1Zn-$MeIm^-$ (ν_{11} in Table 8) with the calculated frequencies of 1357, 1291, and 1333 cm^{-1}, respectively. Experimentally, the metal-bound N3D-Im and metal-bridging Im^- forms showed prominent bands at 1352−1340[6,19,20,30−32] and 1292−1282 cm^{-1},[5,6,18,27,33] respectively (Table 12). These are in good agreement with the calculated frequencies, and thus, these bands can probably be assigned to the above C2N3 and N3C4 mode. The latter band at ~1285 cm^{-1} of the metal-bridging His^- was considered to be upshifted from the intense band at 1257 cm^{-1} of free His^- [5,27] (1255 cm^{-1} in $MeIm^-$ [45]). According to our previous calculations,[45] this mode of free $MeIm^-$ (calculated at 1254 cm^{-1}) is due to the C5H deformation (29%) and the C5N1 (28%) and C2N3 (26%) stretches, while the 1291 cm^{-1} mode of Zn_2-$MeIm^-$ has contributions of the C2N3 (36%) and N3C4 (16%) stretches and the C5H deformation (15%). Thus, the major mode change upon metal binding is participation of the N3C4 stretch instead of the C5N1 stretch, which may partly account for the shift in frequency. To the best of our knowledge, there is no study of Raman markers of the N1Zn-Im^- form in the ring vibrations. We predict that the C2N3 and N3C4 stretching mode of the N1Zn-Im^- form, which was calculated at 1333 cm^{-1}, would show an intense Raman band similar to the corresponding modes in other forms.

The metal-bound N1D-Im form gives a strong band at 1394−1381 cm^{-1} [6,30,32] (Table 12). The assignment of this band is the mixed mode of the CH_3 symmetric deformation (31%) and the N1C2 (21%) and C5N1 (12%) stretches calculated at 1402 cm^{-1} (ν_{11} in Table 4). Miura et al.[30] considered this band to originate from the band at ~1480 cm^{-1} of the corresponding N-protonated form. In fact, the mode calculated at 1470 cm^{-1} in Zn-bound N1H-MeIm has contributions from the N1C2 (29%) and C5N1 (17%) stretches with considerable coupling with the N1H deformation (37%) (ν_9 in Table 3). The large downshift upon N-deuteration is explained by decoupling of the NH vibration. The frequency may be shifted down to the region of the CH_3 symmetric deformation, coupled with this vibration, thus yielding the above mode at 1402 cm^{-1}.

In Zn-bound N3H-MeIm, the mode with a large contribution due to N1H deformation was calculated at 1414 cm^{-1} (N3H deformation (25%), C4C5 stretch (15%), CH_3 asymmetric deformation (14%); ν_{11} in Table 5). This mode was observed at 1434−1425 cm^{-1} with a strong Raman intensity and has been proposed to be a Raman marker of the metal-bound N3H-Im form[22,30] (Table 12).

In both the neutral N1H-Im and N3H-Im forms, a band at 1503 cm^{-1} was often observed upon metal binding.[30−32,40] This band is small in intensity but occurs at a rather isolated position from other bands, and hence it has been proposed to be a marker of metal binding.[30−32,40] The corresponding mode was calculated at 1516 and 1518 cm^{-1} for Zn-bound N1H- and N3H-MeIm, respectively and was assigned to the mixed mode of the N1C2 and C2N3 stretching and C2H deformation vibrations (ν_8 in Tables 3 and 5). This band looks like a new band[30] but actually appeared at this position by upshift of the mode with a major contribution from the C2N3 stretch in the metal-free N1H-form and of the N1C2 stretch in the N3H-form, which was calculated at 1502 and 1494 cm^{-1}, respectively.[45] As mentioned above, metal binding to the neutral 4-MeIm form makes the N1C2N3 structure more symmetric, and the N1C2 and C2N3 stretching vibrations are coupled with each other, thus causing the frequency upshift.

5. Metal−Im Stretching Vibration. Detecting the metal−Im stretching vibration provides direct evidence of metal binding to histidine. The metal−Im stretching vibration has been observed in the 325−200 cm^{-1} region.[13,14,16,23,57] It has been reported that deprotonation of the imidazole ring upshifts the frequency by 25−40 cm^{-1}, and hence, the upshifted frequency can be used as an indicator of deprotonation.[14,16,23] In our calculations, the Zn−Im stretching frequency at 260−255 cm^{-1} for Zn-bound N1H(D)-MeIm and N3H(D)-MeIm (ν_{30} in Tables 3−6) upshifted by ~25 cm^{-1} to 286−280 cm^{-1} upon deprotonation (ν_{26} in Tables 7 and 8). This was consistent with the observed experimental data. The calculations showed that this rule is not applicable to the metal-bridging Im^-, which yielded the split frequencies at 305 and 199 cm^{-1} because of coupling of the two Zn−Im stretches (ν_{26} and ν_{28} in Table 9). However, the presence of two Zn−Im bands with relatively high and low frequencies would differentiate this structure from the others.

Functional Relevance of a Histidine Ligand in Metalloenzymes. The present calculation showed that upon Zn binding to the neutral forms of 4-MeIm the N−H distance increases (Table 1) and the NH stretching frequency decreases (Tables 3 and 5), indicating the increased acidity of the hydrogen atom in the N−H bond. This metal effect is consistent with the previous calculations by El Yazal and Pang,[58] in which the proton dissociation energy of imidazole is reduced upon metal binding. In fact, it has been reported that although the p*K*a of neutral histidine is as high as 14 in the free state metal binding lowers its value,[1] and in some metalloenzymes, the presence of deprotonated histidine ligands has been suggested.[16,35,36] These data imply that a histidine ligand is quite suitable for functioning as a proton donor or acceptor in metalloenzymes.

In the Zn-MeIm complexes, negative charge is partially transferred from the imidazole ring to the Zn^{2+} ion. The decrease in the charge of the Zn^{2+} ion by this effect was ~0.12 e for the neutral forms of 4-MeIm, while this value became ~1.8 times larger when the 4-MeIm ligand was deprotonated (Table 2). This means that the protonation state of a histidine ligand can alter the electronic property of the binding metal ion. When the metalloenzyme in question is a redox enzyme, this change in the electronic property would directly affect the redox potential of the metal center. In addition, the change in the charge of the metal ion might affect the properties of other ligands. Cini et al.[54] previously showed that coordination of an imidazole ring to the metal ion decreases the acidity of the water ligands by the charge neutralization effect. Our calculations showed that deprotonation of a histidine ligand also lowers the acidity of water ligands (Table 2). This effect may be important in controlling the catalytic reactions in some metalloenzymes because ligand water often functions as a proton donor to a substrate. Moreover, effects of the protonation state of histidine on other ligands cannot be limited to water and thus might directly affect the reactivity of a substrate molecule bound to the metal ion.

Acknowledgment. We thank Dr. Hiroshi Yoshida for useful advice about calculation and Dr. Chihiro Kato for providing us the upgraded program of NCTB. Also, we are grateful to Drs. Takashi Miura and Shinji Hashimoto for providing the observed Raman frequencies of Zn−(DL-His)$_2$, Ni−(DL-His)$_2$, and Cu−

(βAla-His) and those of Zn−$(His^{-})_2$ and Zn−$(MeIm^{-})_2$, respectively. This research was supported by grants for the Bioarchitect Research Project and Frontier Research System of RIKEN given by the Ministry of Education, Culture, Sports, Science and Technology of Japan.

References and Notes

(1) Sundberg, R. J.; Martin, R. B. *Chem. Rev.* **1974**, *74*, 471.
(2) Regan, L. *Annu. Rev. Biophys. Biomol. Struct.* **1993**, *22*, 257.
(3) Ascone, I.; Castaner, R.; Tarricone, C.; Bolognesi, M.; Stroppolo, M. E.; Desideri, A. *Biochem. Biophys. Res. Commun.* **1997**, *241*, 119.
(4) Murphy, L. M.; Strange, R. W.; Hasnain, S. S. *Structure* **1997**, *5*, 371.
(5) Wang, D.; Zhao, X.; Vargek, M.; Spiro, T. G. *J. Am. Chem. Soc.* **2000**, *122*, 2193.
(6) Hashimoto, S.; Ono, K.; Takeuchi, H. *J. Raman Spectrosc.* **1998**, *29*, 969.
(7) Morgan, J. E.; Verkhovsky, M. I., Wikström, M. *J. Bioenerg. Biomembr.* **1994**, *26*, 599.
(8) Wikström, M. *Biochim. Biophys. Acta* **2000**, *1458*, 188.
(9) Garfinkel, D.; Edsall, J. T. *J. Am. Chem. Soc.* **1958**, *80*, 3807.
(10) Bellocq, A. M.; Perchard, C.; Novak, A.; Josien, M. L. *J. Chim. Phys.* **1965**, *62*, 1334.
(11) Lord, R. C.; Yu, N.-T. *J. Mol. Biol.* **1970**, *51*, 203.
(12) Yoshida, C. M.; Freedman, T. B.; Loehr, T. M. *J. Am. Chem. Soc.* **1975**, *97*, 1028.
(13) Salama, S.; Spiro, T. G. *J. Am. Chem. Soc.* **1978**, *100*, 1105.
(14) Stein, P.; Mitchell, M.; Spiro, T. G. *J. Am. Chem. Soc.* **1980**, *102*, 7795.
(15) Caswell, D. S.; Spiro, T. G. *J. Am. Chem. Soc.* **1986**, *108*, 6470.
(16) Smulevich, G.; Mauro, J. M.; Fishel, L. A.; English, A. M.; Kraut, J.; Spiro, T. G. *Biochemistry* **1988**, *27*, 5477.
(17) Zhao, X.; Wang, D.; Spiro, T. G. *J. Am. Chem. Soc.* **1998**, *120*, 8517.
(18) Zhao, X.; Wang, D.; Spiro, T. G. *Inorg. Chem.* **1998**, *37*, 5414.
(19) Vargek, M.; Zhao, X.; Lai, Z.; McLendon, G. L.; Spiro, T. G. *Inorg. Chem.* **1999**, *38*, 1372.
(20) Zhao, X.; Chen, R.; Deng, Q.; Mabrouk, P. A.; Spiro, T. G. *Isr. J. Chem.* **2000**, *40*, 15.
(21) Ashikawa, I.; Itoh, K. *Biopolymers* **1979**, *18*, 1859.
(22) Itabashi, M.; Itoh, K. *Chem. Lett.* **1979**, 1331.
(23) Teraoka, J.; Kitagawa, T. *J. Biol. Chem.* **1981**, *256*, 3969.
(24) Tasumi, M.; Harada, I.; Takamatsu, T.; Takahashi, S. *J. Raman Spectrosc.* **1982**, *12*, 149.
(25) Chinsky, L.; Jolles, B.; Laigle, A.; Turpin, P. Y. *J. Raman Spectrosc.* **1985**, *16*, 235.
(26) Asher, S. A.; Murtaugh, J. L. *Appl. Spectrosc.* **1988**, *42*, 83.
(27) Hashimoto, S.; Ohsaka, S.; Takeuchi, H.; Harada, I. *J. Am. Chem. Soc.* **1989**, *111*, 8926.
(28) Takeuchi, H.; Kimura, Y.; Koitabashi, I.; Harada, I. *J. Raman Spectrosc.* **1991**, *22*, 233.
(29) Hashimoto, S.; Takeuchi, H. *J. Am. Chem. Soc.* **1998**, *120*, 11012.
(30) Miura, T.; Satoh, T.; Hori-i, A.; Takeuchi, H. *J. Raman Spectrosc.* **1998**, *29*, 41.
(31) Miura, T.; Satoh, T.; Takeuchi, H. *Biochim. Biophys. Acta* **1998**, *1384*, 171.
(32) Miura, T.; Hori-i, A.; Mototani, H.; Takeuchi, H. *Biochemistry* **1999**, *38*, 11560.
(33) Miura, T.; Suzuki, K.; Kohata, N.; Takeuchi, H. *Biochemistry* **2000**, *39*, 7024.
(34) Berthomieu, C.; Boussac, A.; Mäntele, W.; Breton, J.; Nabedryk, E. *Biochemistry* **1992**, *31*, 11460.
(35) Hienerwadel, R.; Berthomieu, C. *Biochemistry* **1995**, *34*, 16288.
(36) Berthomieu, C.; Hienerwadel, R. *Biochemistry* **2001**, *40*, 4044.
(37) Markham, L. M.; Mayne, L. C.; Hudson, B. S.; Zgierski, M. Z. *J. Phys. Chem.* **1993**, *97*, 10319.
(38) Wellner, N.; Zundel, G. *J. Mol. Struct.* **1994**, *317*, 249.
(39) Majoube, M.; Millié, Ph.; Vergoten, G. *J. Mol. Struct.* **1995**, *344*, 21.
(40) Torreggiani, A.; Bonora, S.; Fini, G. *Biopolymers* **2000**, *57*, 352.
(41) Noguchi, T.; Inoue, Y. *J. Biochem.* **1995**, *118*, 9.
(42) Noguchi, T.; Inoue, Y.; Tang, X.-S. *Biochemistry* **1999**, *38*, 399.
(43) Noguchi, T.; Kurrech, J.; Inoue, Y.; Renger, G. *Biochemistry* **1999**, *38*, 4846.
(44) Noguchi, T.; Inoue, Y.; Tang, X.-S. *Biochemistry* **1999**, *38*, 10187.
(45) Hasegawa, K.; Ono, T.; Noguchi, T. *J. Phys. Chem. B* **2000**, *104*, 4253.
(46) Frisch, M. J.; Trucks, G. W.; Schlegel, H. B.; Scuseria, G. E.; Robb, M. A.; Cheeseman, J. R.; Zakrzewski, V. G.; Montgomery, J. A., Jr.; Stratmann, R. E.; Burant, J. C.; Dapprich, S.; Millam, J. M.; Daniels, A. D.; Kudin, K. N.; Strain, M. C.; Farkas, O.; Tomasi, J.; Barone, V.; Cossi, M.; Cammi, R.; Mennucci, B.; Pomelli, C.; Adamo, C.; Clifford, S.; Ochterski, J.; Petersson, G. A.; Ayala, P. Y.; Cui, Q.; Morokuma, K.; Malick, D. K.; Rabuck, A. D.; Raghavachari, K.; Foresman, J. B.; Cioslowski, J.; Ortiz, J. V.; Stefanov, B. B.; Liu, G.; Liashenko, A.; Piskorz, P.; Komaromi, I.; Gomperts, R.; Martin, R. L.; Fox, D. J.; Keith, T.; Al-Laham, M. A.; Peng, C. Y.; Nanayakkara, A.; Gonzalez, C.; Challacombe, M.; Gill, P. M. W.; Johnson, B. G.; Chen, W.; Wong, M. W.; Andres, J. L.; Head-Gordon, M.; Replogle, E. S.; Pople, J. A. *Gaussian 98*, revision A.7; Gaussian, Inc.: Pittsburgh, PA, 1998.
(47) Becke, A. D. *J. Chem. Phys.* **1993**, *98*, 5648.
(48) Lee, C.; Yang, W.; Parr, R. G. *Phys. Rev. B* **1988**, *37*, 785.
(49) Hay, P. J.; Wadt, W. R. *J. Chem. Phys.* **1985**, *82*, 27.
(50) Shimanouchi, T. *Computer Programs of Normal Coordinate Treatment of Polyatomic Molecules*; The University of Tokyo: Tokyo, Japan, 1968.
(51) Yoshida, H.; Tasumi, M. *J. Chem. Phys.* **1988**, *89*, 2803.
(52) Pulay, P.; Fogarasi, G.; Pang, F.; Boggs, J. E. *J. Am. Chem. Soc.* **1979**, *101*, 2550.
(53) Basch, H.; Krauss, M.; Stevens, W. J. *Int. J. Quantum Chem.* **1987,** *XXXI*, 405.
(54) Cini, R.; Musaev, D. G.; Marzilli, L. G.; Morokuma, K. *J. Mol. Struct.: THEOCHEM* **1997**, *392*, 55.
(55) Glendening, E. D.; Reed, A. E.; Carpenter, J. E.; Weinhold, F. *NBO*, version 3.1 (in Gaussian 98); Gaussian, Inc.: Pittsburgh, PA, 1998.
(56) Reed, A. E.; Weinstock, R. B.; Weinhold, F. *J. Chem. Phys.* **1985**, *83*, 735.
(57) Nakamoto, K. *Infrared and Raman Spectra of Inorganic and Coordination Compounds, Part B*, 5th ed.; John Wiley & Sons: New York, 1997.
(58) El Yazal, J.; Pang, Y.-P. *J. Phys. Chem. B* **1999**, *103*, 8773.